# DEVELOPMENTS IN THE ECMWF ANALYSIS SYSTEM

**Peter Lönnberg**
**European Centre for Medium Range Weather Forecasts**
**Shinfield Park, Reading, U.K.**

## 1. INTRODUCTION

### 1.1 Overview of ECMWF data assimilation activities

A substantial part of the 1988 ECMWF Seminar is devoted to describing the data assimilation activity at ECMWF. The work of the ECMWF data assimilation section proceeds along three well defined projects:

- Continued development of the operational statistical interpolation scheme (OI)

- Improved use of satellite data

- Variational analysis

The use of satellite data is described by Pailleux et al. (1988) and Kelly (1988) in this volume and will not be discussed further in this paper. The variational analysis is described in this volume by Talagrand (1988) and Courtier (1988).

The development of the operational data assimilation system is split in several sub-projects:

**A. Tropical analyses**

- Use of divergent structure functions. These were implemented in January 88 and are described by Undén (1988) in this volume.

- Change of frequency cut-off in diabatic heating specification in the normal mode initialisation (NMI); Heckley, pers. comm.

- Use of OLR data to improve diabatic heating specification in NMI (Puri and Heckley, pers. comm.)

- Typhoon bogusing (Andersson and Hollingsworth, 1988)

**B. Developments to the statistical interpolation scheme**

- Increased effective analysis resolution.

- Use of first-guess at the appropriate time (Vasiljevic, pers. comm.)

- Experiments with a 31 level model in data assimilation (Simmons, Undén and Davies, pers.comm.)

**C. Analysis of surface fields (Vasiljevic, pers.comm.) using successive correction**

- Analysis of SST, snow, soil moisture and precipitation

- Analysis of 2 metre temperature and humidity

This paper concentrates on the developments to the ECMWF statistical interpolation scheme and in particular on the efforts to improve the horizontal resolution of the analysis.

1.2 Background to the analysis resolution work

The effective analysis resolution is determined by the structure functions used in the statistical interpolation scheme, by the observation density and by the data selection algorithms. The upper bound of the analysis resolution is set by the analysis projection grid, i.e. T106 L19 at ECMWF. Four major changes to the forecasting system over the past four years (1984-88) have increased the effective analysis resolution and the upper bound of it: the use of a forecast error correlation model based on a series of Bessel functions instead of a negative squared exponential (Gaussian) model (Shaw et al., 1987); the use of continuous vertical correlations for direct evaluation of increments on model levels (Shaw et al., 1987); the change in model resolution from T63 to T106 (Jarraud et al., 1985); and the use of the model's horizontal representation (T106) instead of the N48 grid together with use of data at reported pressure with the introduction of a new analysis code (Lönnberg et al., 1986) in September 86. The September 86 to July 88 operational version of the analysis system will, for the purpose of this paper, be called the medium resolution analysis (MRA). In July 88 the high resolution analysis (HRA) became operational.

An increase of the effective analysis resolution is supported by the theoretical and empirical work on the 3-D forecast error covariances (Hollingsworth and Lönnberg, 1986; Lönnberg and Hollingsworth, 1986, hereafter called HL and LH). HL/LH showed that there are well defined structures in the background field at scales smaller than the effective resolution of MRA. By verifying the ECMWF analyses against radiosonde data and in

particular by studying observation-minus-analysis covariances, Hollingsworth and Lönnberg (1989) found that the MRA scheme does not, by any means, extract all available information in data rich regions. However, any increase of the analysis resolution leads to a decrease in the effective data density thereby reducing the possibilities of identifying erroneous observations and of suppressing noise.

Improvements to the analysis resolution naturally falls into three categories: horizontal, vertical and temporal resolution. As mentioned above a considerable enhancement of the horizontal resolution of the ECMWF analysis scheme has recently become operational. The comparison of the HRA scheme with the MRA system constitutes a major part of this paper.

The vertical problem is quite different. Any further increase of the vertical analysis resolution, beyond the enhancements introduced with HRA and through the use of divergent structure functions (Undén, 1988) is constrained by the model's vertical resolution. Significant gains in analysis accuracy are expected from an increased vertical resolution in the forecast model. It would then become worthwhile to extract from radiosondes more detail which at present is not used, i.e. significant level data. HL/LH also found that the vertical wind correlations are sharper than the height correlations suggesting that the correlations are not separable in horizontal and vertical parts. With higher vertical resolution in the model and higher data density in the vertical it would become feasible to use non-separable structure functions.

Enhancements in spatial analysis resolution will make the error arising from the mismatch between observation time and analysis time more serious. Technically a fairly straightforward approach would be to increase the data assimilation frequency from 6 hours to 3 hours. However, this would create new problems as a result of the reduction in data density, in particular at intermediate observation times. An alternative approach is to continue with 6 hourly cycling but to calculate the first-guess at the observation times, instead of only at the analysis time. The departure of the observation from the background at the appropriate time would be used assuming that the structure of the forecast error remains unchanged within the six hour analysis window.

The HRA modifications are described in Section 2. A complete revision of the OI statistics has been made based on the performance of the assimilation system in summer 86 and winter 86/87. The main change is the reduced filtering by the analysis scheme at small horizontal scales giving good response to observations in most situations. Very extreme systems, like tropical cyclones, are still not analysed with sufficient detail.

A reassessment of the data usage was found necessary as a result of the changes to the filtering properties of the analysis. Furthermore, the observation error statistics needed to be updated. In addition, the assumption of very low probability of gross observation errors has been relaxed in HRA. Investigations on the performance of different observing systems clearly show that some of them frequently have large errors caused by the observing technique itself or by the processing of the observed signal. For these systems, i.e. cloud track winds, aircraft winds and satellite thicknesses, it has been assumed that a large departure is more likely to be an observation error than in case of radiosondes. Tighter rejection limits have been used in the HRA assimilations for observing systems with a high probability of gross errors.

The impact of the HRA modifications on the data assimilation is discussed in Section 3. The improved response to mass and in particular wind data is clearly evident from statistics on fit to observations and from synoptic evaluation.

Section 4 deals with the forecast response to the HRA scheme. Most forecasts improve in the short range when run from the high resolution analyses. Some rather spectacular gains have been made in the short range, most notably with the October 87 storm. The likely cause for the short range forecast improvements is tought to be the more accurate wind analyses and the more sophisticated QC of wind data in the HRA scheme as compared to MRA. The clearest signal to emerge from the HRA experimentation is the forecast sensitivity in the early medium range to satellite thickness data. A strong coupling between quality control of SATEM data and forecast skill has been found (Pailleux et al., 1988). The forecast sensitivity to (bad) satellite data is much less in MRA. In the Southern hemisphere, the forecasts run from the HRA analyses have clearly higher skill than those run from the MRA analyses.

Section 5 provides a brief description of the envisaged work of improving the vertical analysis resolution by increasing the model resolution, by use of significant level data and by relaxing the requirement of separability of the correlations into horizontal and vertical parts. The use of a first-guess at the appropriate time is also discussed in Section 5.

Section 6 summarizes the main results. The HRA scheme is a necessary prerequisite for proper use of high resolution data sets. Also, the HRA experiments show that sophisticated QC is an essential part of a high resolution analysis system and that further improvements in the quality control algorithms will bring gains in forecast skill.

## 2. DESCRIPTION OF A HIGH RESOLUTION ANALYSIS SCHEME

The theoretical background of the ECMWF mass and wind analysis has been described by Lorenc (1981). Details of the scheme can be found in Lönnberg and Shaw (1987). Recent analysis changes have been documented by Pailleux et al. (1988) and Undén (1988). The HRA modifications constitute a major overhaul of the essential statistics of the ECMWF analysis scheme.

The modifications fall into three groups:

(i) Revised forecast error statistics (horizontal and vertical)
(ii) Reassessment of use and quality of data
(iii) Quality control changes

### 2.1 Revised forecast errors

The assimilation statistics of the MRA system are based on the performance of the system in 1983 (HL/LH). A new set of statistics have been derived from summer 86 (months JJA) and winter 86/87 (DJF) data for use in HRA.

Several changes have been made to the specification of forecast errors in the analysis:

(i) 9 term Bessel function series instead of 6 terms.
The horizontal forecast error covariances are modelled by

$$\langle f,g\rangle = \sum_{n=0}^{N} \mu_n f_n g_n J_0 (k_n r/D) \qquad (1)$$

where $\langle f,g\rangle$ is the covariance of the forecast errors of f and g,
f and g being either height, streamfunction or
velocity potential errors

$f_n$ and $g_n$ are error amplitudes of radial mode n

$\mu_n$ = cross-correlation between f and g for mode n

if f=g then $\mu$=1

if f≠g then abs($\mu$)≤1

$k_n$ = wavenumber of mode n

r = distance

D = "selection" radius

$J_0$ = Bessel function of zero order and first kind

The isotropic covariance model (1) is defined for distances 0 to D. The set of wavenumbers $k_n$ is chosen such that the terms in the expansion form an orthogonal basis. (The term n=0 corresponds to a large scale, constant, term.) The amplitudes $f_n$, $g_n$ and the cross-correlations $\mu_n$ are determined by least squares fit to empirical correlation data for a fixed D which should be larger than any observation-observation distance in the analysis. The (square of the) scale of the correlation function is defined by the negative of the ratio between the function itself and its Laplacian taken at the origin (HL). This scale relates the height error variance to the geostrophic vector wind variance. The ratio between height error and velocity component error gives the 'component' length scale: L = g/f E(z)/E(u). The 'component' length scale will be used in the following discussion.

Data studies show that much of the geographical variation of the horizontal forecast error correlations can be described by changing only L (or D) and keeping the A's fixed globally. This means that the shape of the six hour forecast error spectrum is approximately the same everywhere. When we know D and N it is then possible to determine the truncation of the correlation model, i.e. the analysis resolution, by computing the equivalent global wavenumber of the highest retained radial mode.

In HRA the forecast error spectrum is extended to N = 8 by assuming that the height spectrum decreases as wavenumber to the power -4 between modes 5 and 8. This is somewhat steeper than observed by LH. The maximum distance (D) is reduced to about 2600 km. These parameter values of the Bessel series expansion correspond to a truncation at spherical wavenumber 63. The main motivation for choosing a steeper spectrum is to preserve some of the filtering properties at small scales and to avoid excessive increase of the computational cost. The Bessel function series (1) is approximated in the HRA analysis

code by Pade polynomials. The computational cost of this approximation increases rapidly with increasing N and flatness of the error spectrum.

D, L and the truncation are given in Table below for Northern and Southern hemisphere extratropics and for the Equator.

| | MRA | HRA |
|---|---|---|
| N | 5 | 8 |
| D (NH extra) | 2750 km | 2600 km |
| L | 500 km | 400 km |
| truncation | 38 | 63 |
| D (Equator) | 5500 km | 3900 km |
| L | 1000 km | 600 km |
| truncation | 19 | 42 |
| D (SH extra) | 3300 km | 3250 km |
| L | 600 km | 500 km |
| truncation | 32 | 50 |

with smooth transition between regions.
(In the pre-May 84 scheme L was 600 km in the Northern hemisphere extratropics).

The spectral response properties of the MRA and HRA schemes have been investigated. A 1-dimensional problem, following HL, has been set up with equidistant observations analysing the observed variable at the observation points. The OI weight matrix has then the following form

$$\underline{\underline{W}} = \underline{\underline{P}} (\underline{\underline{P}} + \underline{\underline{D}})^{-1}$$

where $\underline{\underline{P}}$ and $\underline{\underline{D}}$ are the prediction and observation error covariances between the observation points. In this exercise it has been assumed that the observation errors are uncorrelated and of equal magnitude, i.e. $\underline{\underline{D}} = \sigma^2 \underline{\underline{I}}$ , where $\underline{\underline{I}}$ is the identity matrix. Decomposition of the weight matrix into its eigenvalues and vectors describes the analysis

response to different structures in the input. The eigenvalues give the ratio of output to input for each mode.

The distance between the endpoints of the domain is chosen to 800 km, which corresponds closely to the (1-D) extent of the data selection in a relatively data dense area. The response is expressed as function of data density. Only the response of the gravest modes is considered here and modes which are almost competely damped are not discussed. The dimension of the eigenvalue problem depends on the number of observations involved. However, the structures of the gravest modes change very little with data density and therefore it is possible to compare the response properties for different data densities.

Fig. 1 shows the eigenvectors for MRA; those for HRA are very similar. The gravest mode (mode 1) is roughly constant in the domain, while mode 2 is the linear trend through the domain. Each higher mode has one more zero in the domain. The data density is varied between 200 km (5 observations) and 20 km (41 observations). With increasing number of data, the sum of the weights given to the observations increases, thereby improving the response to all modes.

Comparing MRA with HRA, there is almost no difference in the response to modes 1 and 2 (Figs. 2a and b). Mode 3 (half wavelength 400 km) has a somewhat weaker response in MRA than HRA. The most marked change in the response occurs for mode 4 (half wavelength 267 km) which is reasonably well resolved in HRA, but strongly damped in MRA. Mode 5 (200 km) is almost completely removed in MRA, while the HRA scheme returns a strongly damped mode 5. The heavy damping starts at half wavelengths shorter than 400 km in MRA and 300 km in HRA.

The dependence of the response on the assumed observation errors has been studied. The impact of reducing the normalised observation error from 0.5 to 0.25 is strong for modes which have clearly non-zero eigenvalues (Fig. 3). In MRA, mode 5 is strongly damped even when the observation error is 0.25. Even when the error is reduced to 0.1 (not shown) mode 5 is still strongly damped. In the ECMWF analysis scheme, the normalised observation error is required to be at least 0.33.

Although it has been possible to determine the forecast error correlations for significantly smaller scales than are now proposed (HL) a further increase in the resolution of the structure functions would not be compatible with the data density and quality over most parts of the globe (Bengtsson, 1988). Setting the truncation at global wavenumber 63 required considerable efforts in designing QC algorithms which are compatible with the HRA resolution.

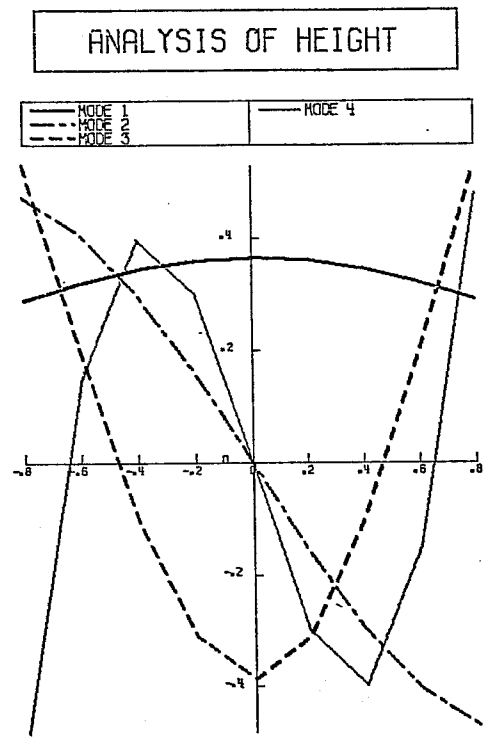


Fig. 1 The four gravest eigenvectors of the response by the MRA scheme for an observation density of 100 km and with a normalised observation error of 0.5.

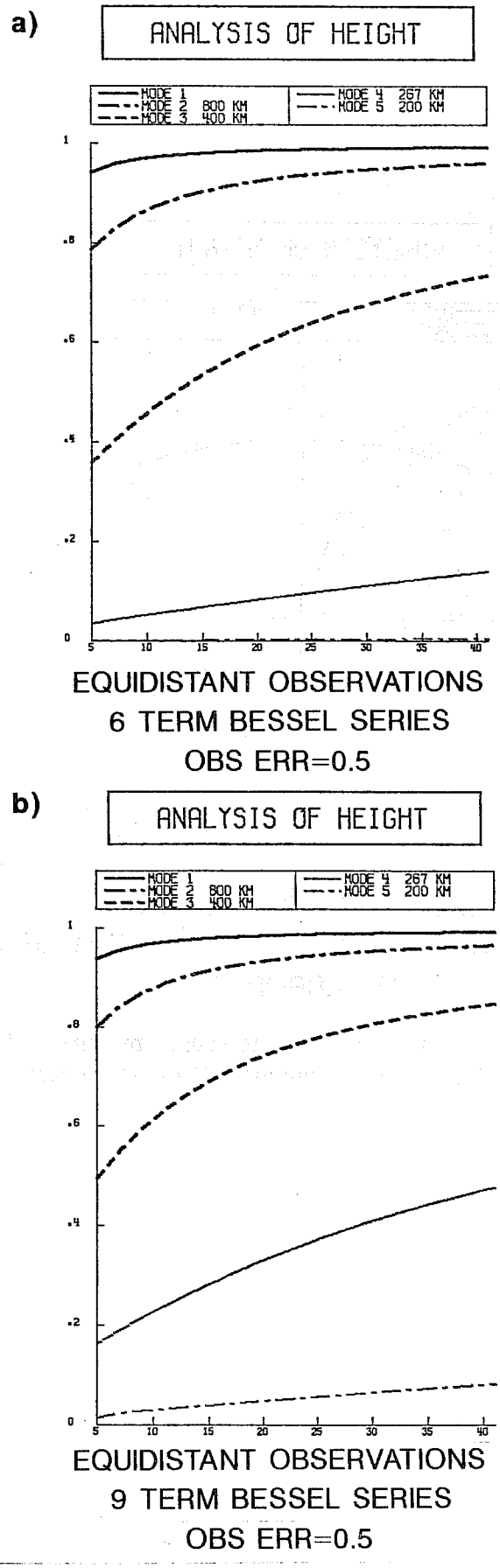


Fig. 2 Eigenvalues of the weight matrix for MRA (a) and HRA (b) for the five gravest modes as function of number of observations in the 800 km domain. The normalised observation error is 0.5.

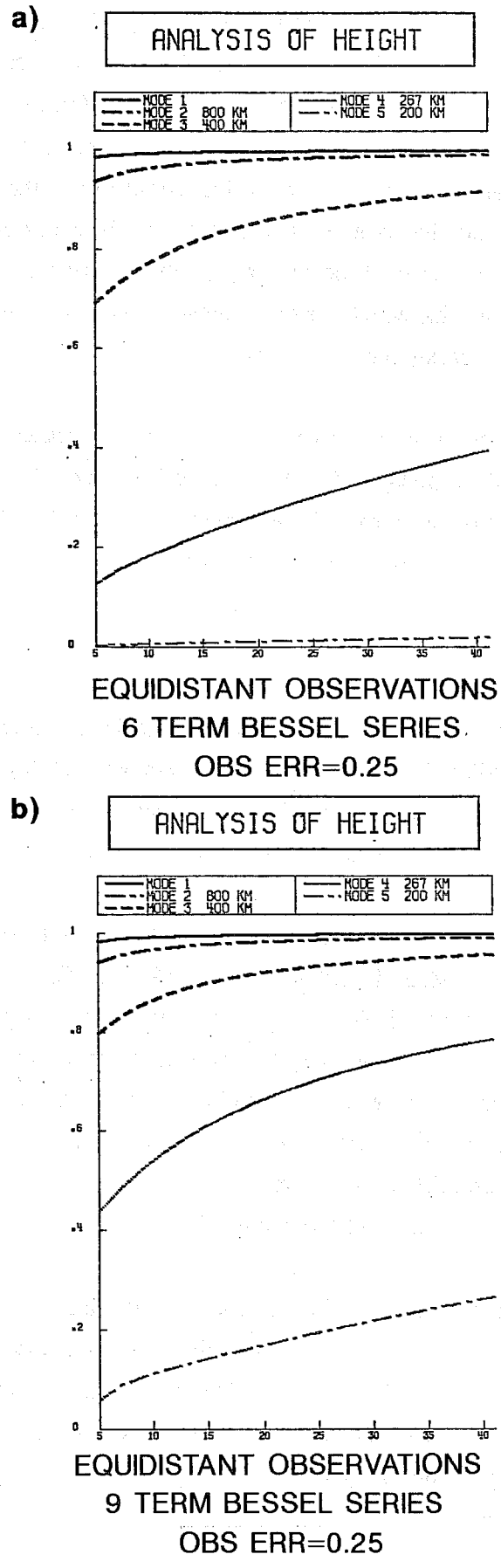


Fig. 3 Same as Fig. 2, but for a normalised observation error of 0.25.

The forecast error spectrum influences the calculation of the OI analysis error estimate. Only those scales which are explicitly resolved by the forecast error correlations can have analysis errors. Scales which are not resolved by the structure functions have no forecast errors by definition and therefore no analysis errors. As more and smaller scales are resolved by the HRA correlations than by the MRA correlations, the OI analysis error estimate contains more scales and the total error variance then becomes larger in HRA than MRA. As the estimated analysis error becomes larger, the subsequent (six hour) forecast error estimates increase. This increased error together with a reduced length scale increases significantly the assumed background error for the wind.

The OI algorithm estimates the analysis error on the resolved scales. The error of the unresolved scales is provided explicitly for the OI check and for the forecast error estimation. At 1000 hPa the analysis error of the unresolved scales has been estimated to 6 m for height in MRA (Shaw et al., 1984). In the HRA scheme it has been reduced to 5 m as more scales are resolved.

(ii) Scale dependence of geostrophic coupling

The coupling between the height and the streamfunction fields is independent of scale in MRA. However, empirical studies (LH) indicate that the coupling at higher wavenumbers is quite weak. Furthermore, the wind observations are more useful than the observed inter-station height gradients to describe fine details in the flow.

In HRA, the five gravest modes have a height-streamfunction correlation of 0.9 ($\mu_{1\text{-}5}$) in Northern hemisphere extratropics, while in MRA $\mu_{1\text{-}5}$ is 0.95. In HRA, mode 6 ($\mu_6$) has a correlation of 0.45 and modes 7 and 8 ($\mu_{7\text{-}8}$) have no geostrophic coupling at all. On the smallest resolved scales the wind and the height analyses are then independent. According to geostrophic adjustment theory, the wind information is retained on the smallest scales and the mass field adjusts to the wind, which agrees well with the relative data representativeness. A 2 day assimilation with two 10 day forecasts showed a mildly positive response to loosening of the height-streamfunction coupling from 0.95 to 0.90.

(iii) Use of fast approximations to Bessel functions by Pade polynomials

In MRA the Bessel functions are approximated by series of Tschebyscheff polynomials. To obtain the necessary accuracy for the 9 term Bessel series, it would have become prohibitively expensive to use an approximation by Tschebyscheff polynomials. A fast and accurate approximation using Pade polynomials (ratio of two polynomials) has been developed (Hollingsworth, pers.comm.):

$$f(r) = \frac{\sum_{i=1}^{35} a_i \, r^i}{1 + \sum_{i=1}^{35} b_i \, r^i} \qquad (2)$$

(iv) Revised vertical forecast error correlations

Using the most recent assimilation statistics, new vertical correlations have been derived for winter and summer extratropics as well as for the Tropics. The most significant change is in the stratosphere following the introduction of the 19 level model in May 86. Otherwise, the scale height of the tropospheric correlations has been slightly reduced.

(v) Wide vertical correlations over Eastern Pacific

The largest six hour forecast errors in the Northern hemisphere occur in the Eastern Pacific. Due to poor data coverage, the growth of small errors, originating in the Western Pacific, is difficult to suppress while they cross the Pacific. Verification of the 6 hour forecasts against aircraft winds clearly shows that the perceived forecast errors are much lower over the Western Pacific (Fig. 4) than over the Eastern Pacific (Fig. 5). The dashed line in the Figures is the linear regression line of the magnitude of the vector wind difference (observation-minus-forecast) as function of observed wind speed.

In data rich regions, the six hour forecast error consists mainly of an ensemble of small scale modes with fast growth rates. In the Pacific area larger modes, with slower growth rates, have sufficient time to grow in the assimilation to make a significant contribution to the first-guess error. From empirical observation-minus-forecast covariances it can be verified that the vertical correlations over the Eastern Pacific and the North American West Coast are significantly wider than the North American continental correlations. Wide vertical correlations are specified over the Eastern Pacific in HRA.

2.2 Revised observation errors

Significant changes have been made to the observation errors, again based on the latest statistics. The old and new values are given in Tables 1 and 2.

(i) Radiosonde winds

The tropospheric values of the wind errors remain almost unaltered, while the stratospheric errors have been reduced. The use of the 19 level model (since May 86) in the assimilation reduced the perceived 6 hour forecast errors of wind in the stratosphere. In MRA, the

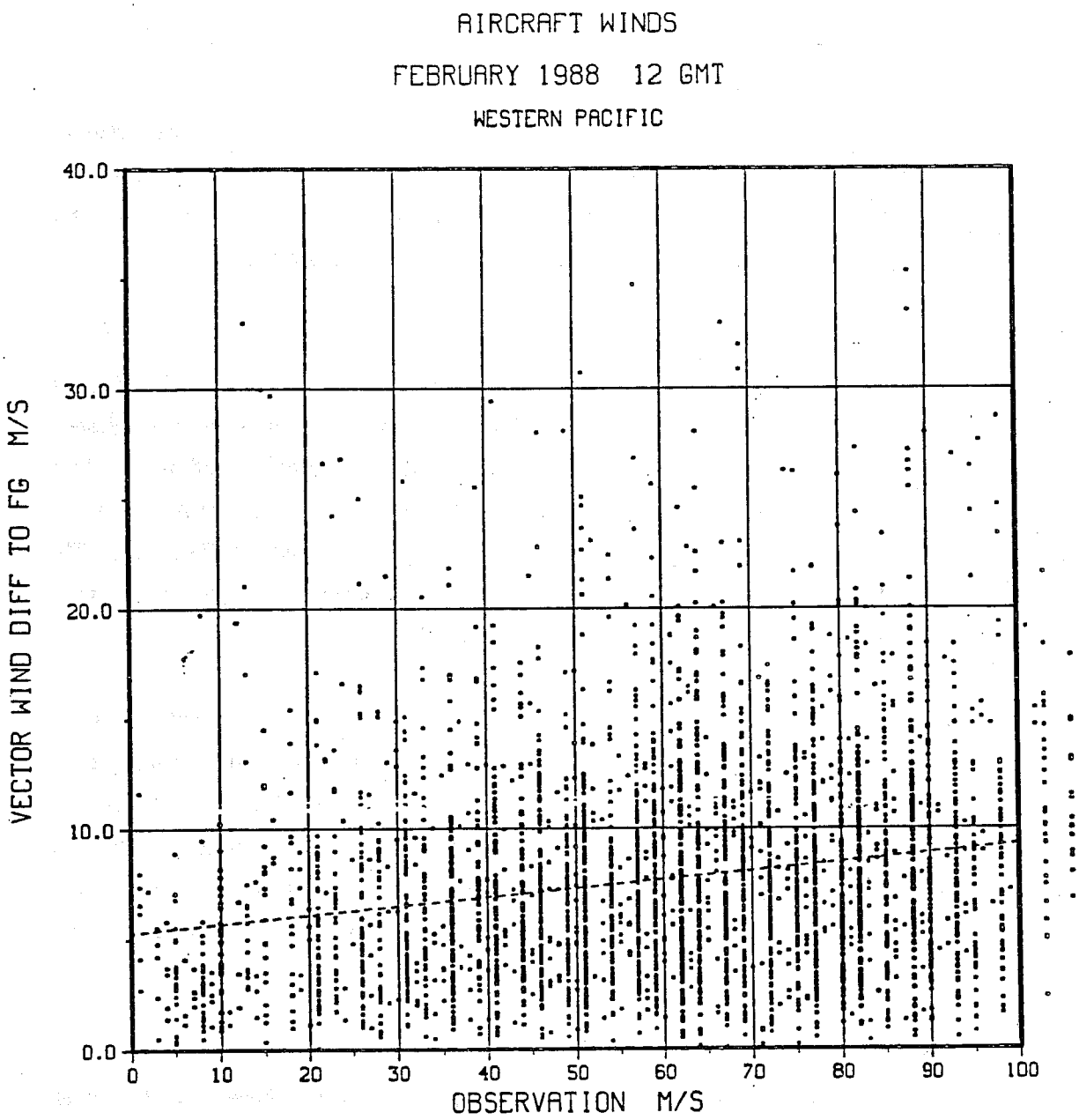


Fig. 4 Scatterdiagram of perceived wind forecast error as verified against aircraft winds in February 1988 12 UTC for Western Pacific. The abscissa is the observed wind speed and the ordinate gives the magnitude of the vector wind difference between observation and 6 hour forecast. The dashed line is a linear regression through the data points.

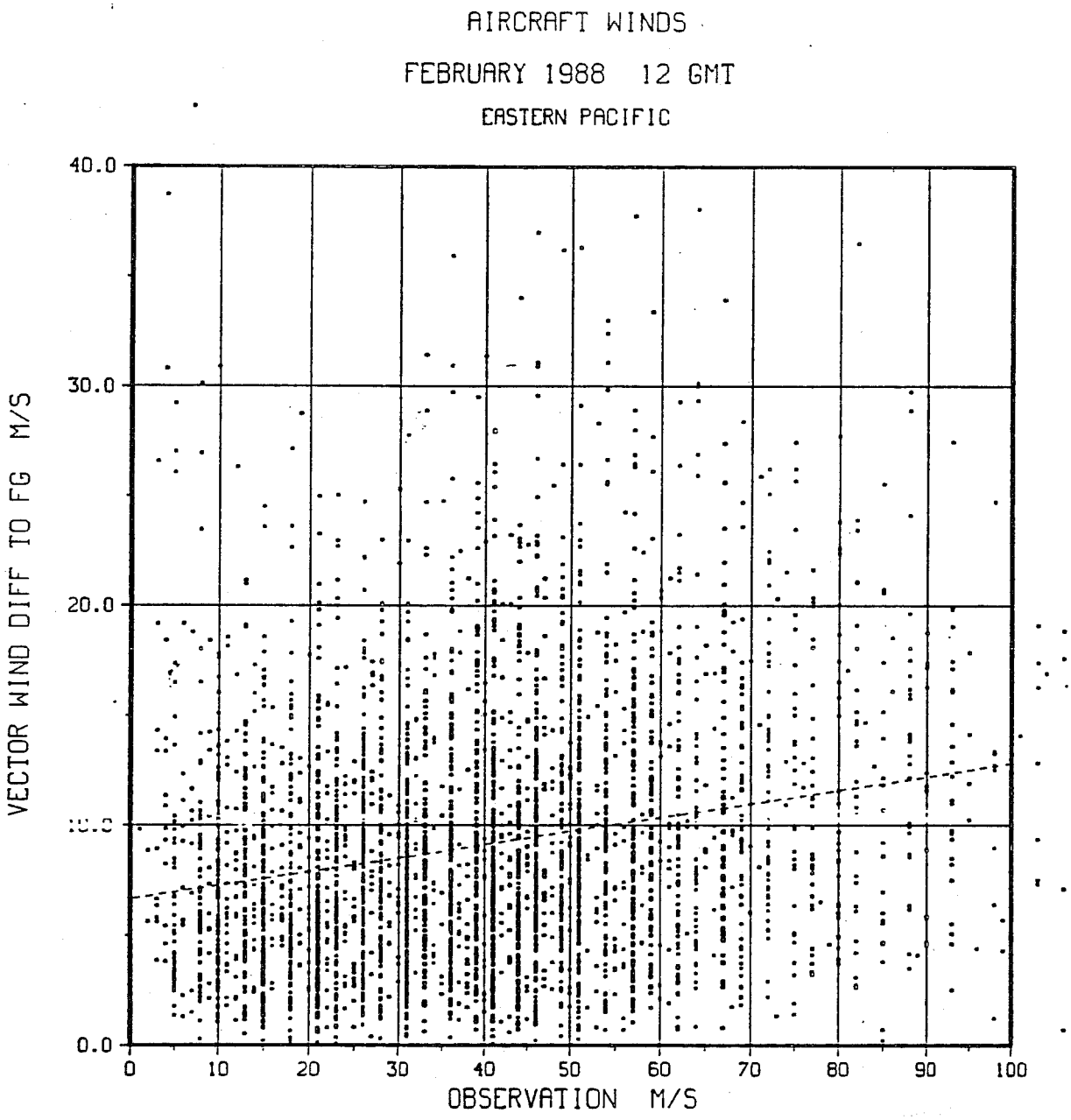


Fig. 5 Same as Fig. 4, but for Eastern Pacific.

Table 1. MRA observation errors

| | TEMP z (m) | TEMP u/v PILOT u/v (m/s) | AIREP (m/s) | SATOB (m/s) |
|---|---|---|---|---|
| 1000 | 5.0 | 2.2 | 3.5 | 2.5 |
| 850 | 5.4 | 2.5 | 3.5 | 2.5 |
| 700 | 6.0 | 2.6 | 3.5 | 2.5 |
| 500 | 9.4 | 3.1 | 3.5 | 2.5 |
| 400 | 11.6 | 3.7 | 3.5 | 5.0 |
| 300 | 13.8 | 3.8 | 4.0 | 5.0 |
| 250 | 14.2 | 3.3 | 4.5 | 5.0 |
| 200 | 15.2 | 3.0 | 5.0 | 5.0 |
| 150 | 18.2 | 2.8 | 5.0 | 5.0 |
| 100 | 21.4 | 2.4 | 5.0 | 5.0 |
| 70 | 25.2 | 2.4 | 5.0 | 5.0 |
| 50 | 29.8 | 2.4 | 5.0 | 5.0 |
| 30 | 31.2 | 2.5 | 5.0 | 5.0 |
| 20 | 38.1 | 3.1 | 5.0 | 5.0 |
| 10 | 50.0 | 3.5 | 5.0 | 5.0 |

SHIP p/z 7.0 m

Land SYNOP p/z 7.0 m

All TEMP heights are assumed to be of the same quality.

Table 2. Observation errors used in HRA experiments

| | TEMP z | | | TEMP u/v PILOT u/v | AIREP | SATOB |
|---|---|---|---|---|---|---|
| | cat 1 (m) | cat 2 (m) | cat3 (m) | (m/s) | (m/s) | (m/s) |
| 1000 | 4.3 | 6.5 | 8.6 | 2.0 | 3.0 | 3.0 |
| 850 | 4.4 | 6.6 | 8.8 | 2.4 | 3.0 | 3.0 |
| 700 | 5.2 | 7.8 | 10.4 | 2.5 | 3.0 | 3.0 |
| 500 | 8.4 | 12.6 | 16.8 | 3.4 | 3.0 | 3.0 |
| 400 | 9.8 | 14.7 | 19.6 | 3.6 | 3.5 | 6.0 |
| 300 | 10.7 | 16.1 | 21.4 | 3.8 | 4.0 | 6.0 |
| 250 | 11.8 | 17.7 | 23.6 | 3.2 | 4.0 | 6.0 |
| 200 | 13.2 | 19.8 | 26.4 | 3.2 | 4.0 | 6.0 |
| 150 | 15.2 | 22.8 | 30.4 | 2.4 | 4.0 | 6.0 |
| 100 | 18.1 | 27.2 | 36.2 | 2.2 | 4.0 | 6.0 |
| 70 | 19.5 | 29.3 | 39.0 | 2.0 | 4.0 | 6.0 |
| 50 | 22.5 | 33.8 | 45.0 | 2.0 | 4.0 | 6.0 |
| 30 | 25.0 | 37.5 | 50.0 | 2.0 | 4.0 | 6.0 |
| 20 | 32.0 | 48.0 | 64.0 | 2.5 | 4.0 | 6.0 |
| 10 | 40.0 | 60.0 | 80.0 | 3.0 | 4.0 | 6.0 |

SHIP p/z 14.0 m

Land SYNOP p/z 7.0 m

Cat 1 = North America ( 80 - 30 N , 50 - 170 W )
Cat 2 = all, except Cat 1 and Cat 3
Cat 3 = South America ( 10 N - 60 S , 30 - 90 W )
Africa, Arabia ( 30 N - 40 S , 20 W - 60 E )

Only observation errors which are different in MRA and HRA have listed in the Tables 1 and 2.

stratospheric wind errors were inflated to lessen the impact of inconsistencies between the persistence first-guess (pre-May 86 system) and observations. With dynamical control of the stratospheric assimilation, proper observation errors can be used in HRA.

(ii) Aircraft reports

The RMS errors of aircraft reports have been reduced based on the latest statistics. Aircraft observations have a much stronger impact in HRA than MRA, due to increased response to wind data in HRA. To avoid adverse effects from erroneous AIREPs in HRA, a conditional first-guess check has been devised to quality-control such data (See Section 2.3.2).

(iii) Satellite winds

A wealth of evidence on the poor quality of satellite winds has been produced at ECMWF (Böttger and Radford, 1988) and elsewhere. In HRA, the influence of these winds has been strongly reduced. A tough conditional first-guess check eliminates a substantial amount of cloud wind data. For the remaining observations the RMS errors have been increased according to the latest statistics.

In HRA, aircraft reports are regarded as more accurate than cloud winds, while the opposite is assumed in MRA.

(iv) Area dependent radiosonde height errors

For radiosonde heights, the observation errors are specified in three quality categories depending on region. The highest quality of heights is assumed over North America, while Africa, Arabia and South America have the poorest height measurements. The ratio of RMS errors is 1 : 1.5 : 2 for good, medium and low quality radiosondes.

## 2.3 Quality control

Quality control of data at ECMWF consists of a chain of checks of increasing severity. Only data which pass the whole sequence of checks are used to calculate analysis increments. Basically, if a datum fails a test, its progress stops at that point. The ECMWF QC principles differ significantly from Gandin's Comprehensive QC (1988) in which the decision to reject or accept (or modify) a datum is based on the results of several tests.

At ECMWF, data are checked at the report decoding stage and by the analysis. At the report decoding level, observations are checked against climatological limits. Also, geopotential and temperature data are tested for hydrostatic consistency. Single error

detection and correction and multiple error detection is an integral part of the hydrostatic check. In the analysis code itself the tests are performed against the background field and against an independent analysis. Both tests have been modified for HRA. The analysis (OI) check has only been tuned to produce similar responses in MRA as in HRA. Most of the QC efforts in HRA have been put on improving the first-guess check. The biggest change between MRA and HRA is the relaxation of the assumption that all observing systems have a very low probability of gross errors.

### 2.3.1 Tuning of first-guess and OI rejection limits

Initially, the high resolution structure function experiments were run without any tuning of the rejection limits of the first-guess and the OI checks. The OI estimate of the analysis errors increases as more scales are resolved by the structure functions. The OI rejection limit is set at n times the sum of the analysis error (squared) and observation error (squared). Any increase in the estimated analysis error makes the OI check more tolerant.

The increased analysis error in turn leads to higher estimated errors of the six hour forecast. Furthermore, the reduced forecast error scale length increased the wind errors to values which rendered the first-guess wind check almost useless. Some forecasts were run from the test assimilations without QC tuning. The results from these forecasts are reported in Section 4.1.

In MRA, the analysis rejects too few observations and only in very fast developments are good data rejected. Accepting and using noisy data when the analysis scheme strongly filters large deviations may not be too serious, but when the filtering is reduced bad data start to have detrimental impact. The first-guess and OI rejection criteria have been tuned in such a way that those data rejected in MRA would also be rejected by HRA. For certain observing systems a more refined quality control has been introduced in HRA.

### 2.3.2 Conditional first-guess check

The area with the largest analysis errors in the Northern hemisphere is the Eastern Pacific. As a result the least accurate six hour forecasts occur near the North American West Coast. The radiosonde data in this area are of good quality which makes it possible to estimate the six hour forecast error. From the distribution of the observed-forecast values it is possible to define the extremes of the first-guess error. These values can then be used to set the first-guess rejection limits. For observing systems which have a very low probability of gross errors this should be a satisfactory basis for quality control.

If, however, a significant proportion of the reports from a station or observing system are corrupted by gross errors, it becomes necessary to set the rejection limits to values for which the probability of gross errors roughly equals that of a large random (normally distributed) difference between report and background (Lorenc and Hammon, 1988).

Special tests have been set up in HRA to handle gross observation errors and non-Gaussian distribution of the background error:

- cloud track winds
- aircraft winds
- satellite thicknesses (Pailleux et al., 1988)
- the skewed distribution of the six hour forecast error of surface pressure

The motion of the air is difficult to estimate from cloud movement in dynamically active regions, like jets. Collocation studies with radiosondes and aircraft data suggest that some of the large SATOB first-guess departures may be corrupt data and should not be used. If such winds are much weaker than the first-guess they are likely to have been derived in an improper way and must then be regarded as having gross observation errors.

A conditional test on cloud winds was implemented in December 1987. The more stringent rejection limits only apply (in MRA) to upper level extratropical SATOB winds which are weaker than the first-guess in a strong background flow (Pailleux, pers.comm.). The test is then asymmetric in that it rejects SATOB winds slower than the first-guess more readily than those SATOB winds which are stronger than the guess. In HRA, the conditional test has been extended to all cloud winds. The test is still asymmetric but positive departures also have a fairly stringent rejection limit.

Aircraft observations have a large probability of gross errors arising from position and time errors. More stringent first-guess rejection limits have been introduced for this data type. Even in the case when a large discrepancy between an aircraft observation and forecast is caused by a forecast error, it may not be advisable to use that single level datum because of incomplete knowledge of the 3-D structure of the forecast error in that particular (extreme) situation. This argument suggests tougher rejection limits for single level data than for multilevel data.

The rejection limits have been set in such way that they in data sparse regions are about 40 m/s for the vector wind difference between TEMP observation and guess (upper level), 28 m/s for aircraft winds (this number agrees well with the results from a statistical study

by Hollingsworth and Rubli on the distribution of the AIREP-minus-forecast values) and 14 m/s for satellite winds and 10 m/s for extratropical upper level satellite winds in jets which are weaker than the first-guess. The analysis code uses non-dimensional rejection limits expressed in standard deviations (STD) of the observation-minus-guess distribution. The dimensional numbers given above translate to 4.2 STDs for TEMPs and PILOTs, 2.4 STDs for aircraft winds, 1.3 STDs for cloud winds and 0.95 STDs for the special category SATOBs.

The changes to the first-guess rejection limits since May 84 are listed in Table 3. The strong tightening of limits for single level wind data is obvious from Table 3.

### 2.3.3 Asymmetric first-guess check of surface pressure data

Surface pressure departures exhibit a skewed distribution towards negative observation-minus-background departures in the storm tracks (Gustafsson and Pailleux, pers.comm). For extratropical (polewards of 30 degrees) near-surface height and pressure data, the first-guess tolerance has been increased for negative departures when the first-guess pressure is low (PMSL < 1000 hPa). The normal (non-dimensional) first-guess rejection limit of 6 STDs, which corresponds approximately to 100 m in data rich regions, is changed to a dimensional limit of 150 m. These observations are then given a further chance in the OI check to survive if they find support from nearby data.

Further improvements in quality control will require more sophisticated techniques and new independent information.

## 3. IMPACT ON ASSIMILATION

### 3.1 Analysis of small scale structures

The reduced filtering at small scales is clearly seen in the fit to observations, in particular to wind data. Fig. 6 shows the RMS difference between the observed zonal wind and analysis for the HRA and MRA systems in 8 assimilation cycles. The fit is very close to theoretical optimum (Hollingsworth and Lönnberg, 1989).

In areas of sonde data, jets are analysed to finer detail in HRA as compared to MRA. According to geostrophic adjustment theory the small scale wind survives the initialisation, while the height field is modified to balance the wind fields. In general, the analysed systems are more intense in HRA than in MRA.

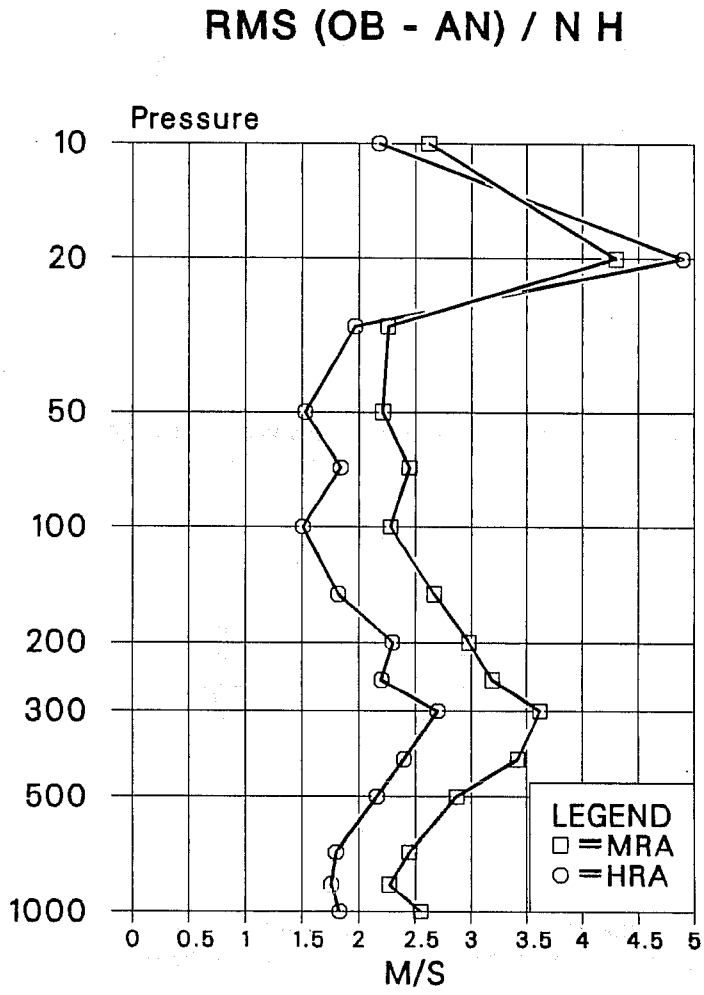


Fig. 6 Time mean (1.2.87-8.2.87 12 UTC) RMS fit of uninitialised analyses to Northern hemisphere radiosonde zonal winds, for MRA and HRA.

Table 3 The evolution of the first-guess rejection limits in 1984-88. The limits are given in terms of standard deviations of the distribution of observation-minus-background.

| | May 84 | Dec 87 | Jul 88 |
|---|---|---|---|
| Winds | | | |
| TEMP standard level | 5.7 | 4.5 | 4.5 |
| significant level | 4.2 | 4.2 | 4.2 |
| AIREP | 4.2 | 4.2 | 2.4 |
| SATOB neg dep jet level | 4.2 | 1.6 | 0.95 |
| all others | 4.2 | 4.2 | 1.3 |
| Heights | 8.0 | 8.0 | 6.0 |

Table 4 Standard deviation of difference between North American observations and six hour forecast for MRA and HRA.

| pressure (hPa) | MRA (m) | HRA (m) |
|---|---|---|
| 700 | 11.0 | 10.5 |
| 500 | 14.6 | 14.2 |
| 250 | 19.9 | 19.1 |
| 100 | 20.9 | 20.7 |
| 50 | 23.5 | 23.1 |

Table 5 Standard deviation of six hour forecast error over North America for MRA and HRA assimilations.

| pressure (hPa) | MRA (m) | HRA (m) |
|---|---|---|
| 700 | 9.8 | 9.1 |
| 500 | 11.9 | 11.3 |
| 250 | 17.3 | 17.0 |
| 100 | 13.0 | 12.2 |
| 50 | 12.6 | 11.8 |

As an example, Figs. 7a and b show the observed and analysed wind for HRA and MRA over the West Coast of North America at 12 UTC February 1 1987. The first guess for this analysis underestimated the strength of the flow and the vertical shear. The analysed jet over Vancouver Island and Washington state is sharper and stronger in HRA. Also,the vertical structure of the wind field has improved which is evident from maps of the wind shear and temperature (Figs. 8a and b).

The HRA scheme has some success in analysing tropical cyclones in terms of intensity and position. The fine detail survives the initialisation and the six hour forecast maintains the additional information in the mass field (Puri, pers. comm.). Promising results in analysing tropical cyclones with the HRA scheme using bogus observations have been obtained by Andersson and Hollingsworth (1988).

### 3.2 Short-range forecast errors

The accuracy of the short-range forecast has been verified against radiosondes over 10 analysis cycles (30 Jan 87 - 8 Feb 87 12 UTC). Although the wind field is analysed to finer detail, the RMS six hour wind f/c errors remain unchanged. For the height field there is consistent reduction of the standard deviation of the difference between observation and first-guess or total error (See Table 4). The total error has been split into observation and prediction errors by extrapolation of observation-minus-forecast correlations to zero distance (HL). Table 5 lists the error of the six hour forecast over North America for HRA and MRA. A substantial part of the MRA six hour height forecast error has a very large horizontal scale. The reduction of the height forecast error seen in HRA has largely occured on the largest scales.

Although the analysis system removes the large scale forecast error in MRA it reappears in the initialised fields. This strong rejection of near surface height information in MRA is much less pronounced in HRA. One possible explanation might be that in MRA the near surface height data receives a high weight compared to upper tropospheric height data and all wind data. This combined with relatively wide vertical correlations leads to a situation in which the near surface height information controls the tropospheric analysis. In HRA, the weight given to height data is slightly reduced and the vertical correlations are sharper. This makes the influence of data more localised.

### 3.3 Discussion of analysis impact of low data quality and QC differences

In the HRA system the continental areas are still sufficiently dense for the OI QC algorithm to detect corrupt observations. Over the oceans the data density compared to the scale length of the structure functions is frequently so low that the QC decisions become less reliable. The use and QC of wind data, in particular single level data over oceans, is of

a)

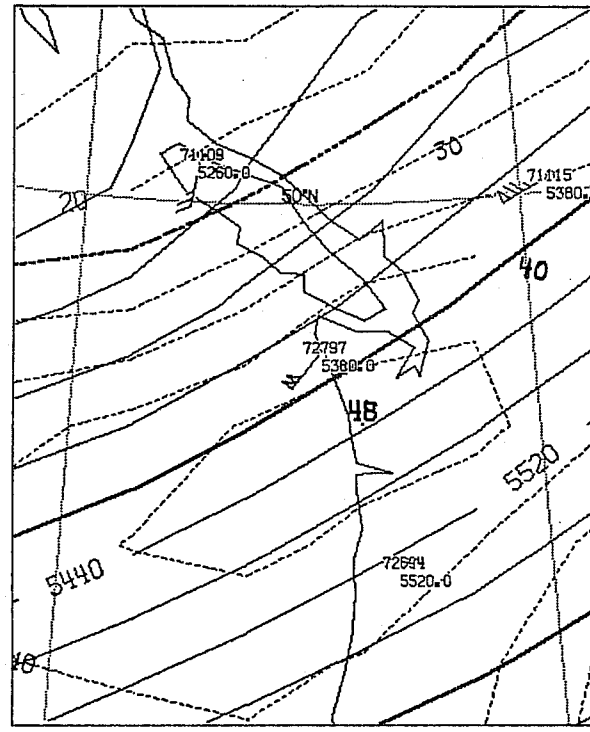


Fig. 7a Analysed 500 hPa height (solid) and wind speed (dashed) for 1 February 1987 12 UTC for MRA with radiosonde observations.

b)

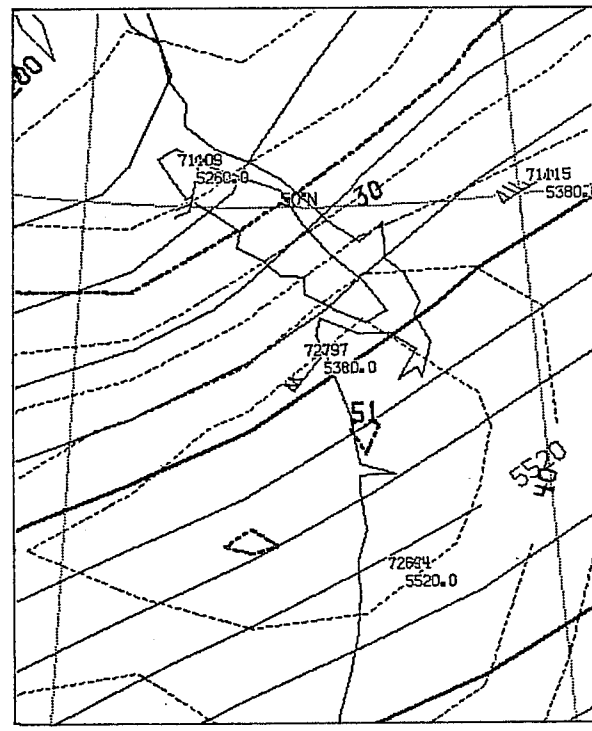


Fig. 7b Same as Fig. 7a, but for HRA.

a)

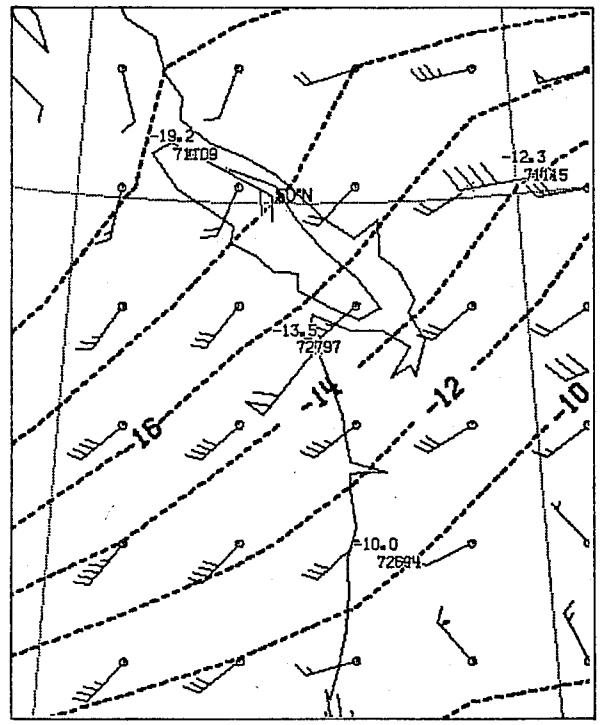


Fig. 8a 500-700 hPa analyses of mean temperature (dashed) and wind shear (wind flags on regular grid) at 1 February 1987 12 UTC for MRA.

b)

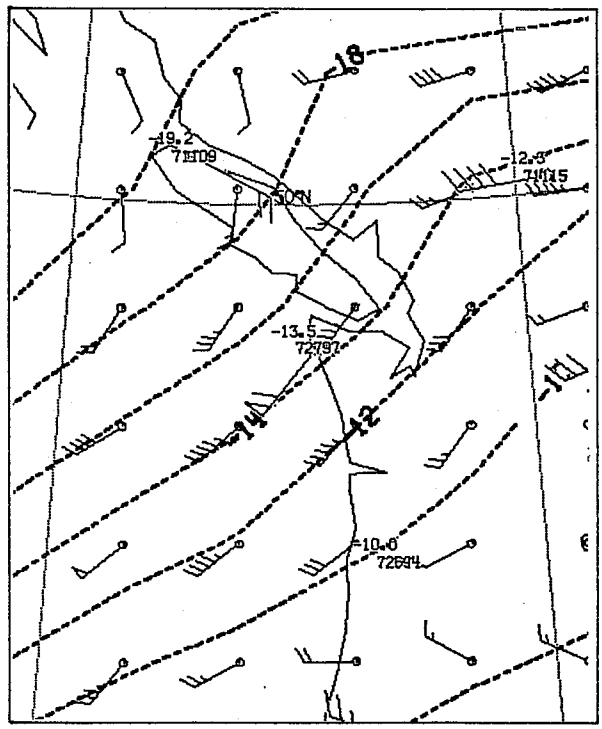


Fig. 8b Same as Fig. 8a, but for HRA.

great importance for medium range forecasting. Differences in QC are responsible for some of the large analysis and forecast differences between HRA and MRA. Such differences can persist in the assimilation for a long period. One such feature originated from different QC decision on winds from Midway Island (28 N, 177 W) and a day later, in the eastern Pacific, the central pressure in a cyclone showed a 5 hPa discrepancy between the two assimilations. During that period the rejections of surface pressure data were identical in that region for the two assimilations. The distressing aspect is that the available information over the Pacific is not plentiful enough to control the analysis of surface pressure. There is also clear evidence that poor quality satellite thicknesses are responsible for large analysis differences over the Pacific.

## 4. FORECAST EXPERIMENTS

This section describes the results from the experiments leading to the final HRA version as well as the forecasts from the final scheme. Much time has been spent on trying to understand the forecast sensitivity to the two analysis schemes. In particular, the causes of poor HRA forecasts have been investigated thoroughly.

### 4.1 General tuning of rejection levels

Three versions of the quality control tolerances have been tested on the period 30 January - 3 February 87. During this period satellite thicknesses were of poor quality. Rapid developments over the eastern Pacific lead to large errors in the six hour forecasts as a result.

The first version of HRA used the MRA QC limits and lead to 25 % reduction in rejections compared to MRA. This QC version of HRA will be called loose QC. The version which best approximates MRA rejection amounts is called medium QC. A third version with 25 % more rejections than in MRA has been tested (tough QC). Changing the QC limits had little impact on rejections of satellite thickness data.

The medium and the tough QC forecasts are more similar to each other than to the loose QC forecasts. In the mean there is little difference in forecast skill between the three versions in the Northern hemisphere. The individual forecasts show considerable variations in skill from day to day. The forecast from the 1 February 87 (Fig. 9) improved clearly with increased rejections, while the forecast from the day after became worse with tougher QC. A plausible explanation to this contradiction might be the quality of the satellite thickness data relative to the first-guess and other observation types. Over the oceans, the QC decisions are largely controlled by the huge amount of satellite thickness data. High quality satellite data should be beneficial to QC, while poor quality satellite data might produce erroneous rejections of good data. One would then expect that the forecast

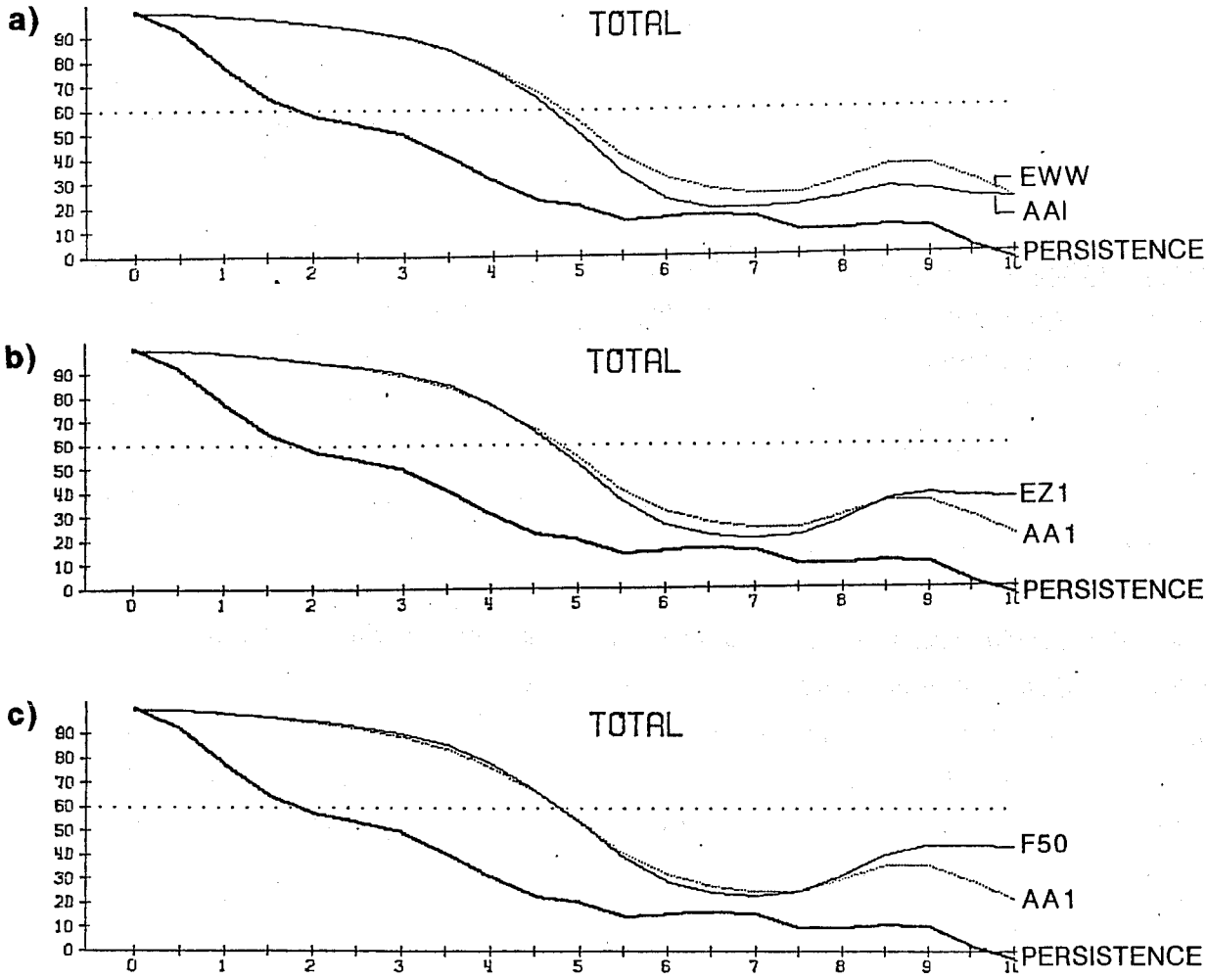


Fig. 9 Anomaly correlation for Northern hemisphere height for forecast from 1 February 1987. In all three figures the dotted line is the operational forecast. The solid lines are correlations for forecasts from HRA assimilations with loose QC (a), medium QC (b) and tough QC (c).

response improves with tighter QC when satellite data is good and the opposite when satellite data is poor. In the four forecast that have been run this appears to be the case.

In the Southern hemisphere, loose QC is clearly detrimental for the forecasts, while forecasts from medium and tough QC are about equal in skill (Fig. 10).

However, this type of simplistic tuning should be used only to remove clearly erroneous observations. Based on the forecast results from the general QC tuning and on detailed investigations of rejections, the final QC version of the HRA scheme was tuned to reject slightly more data than MRA (not counting the additional data rejected by the conditional first-guess checks).

4.2 7-layer satellite processing vs. 11-layer satellite processing

The first HRA experiments were run with the February 87 system as control. That system used the satellite thicknesses in 11-layers as input. Furthermore, that version of the analysis had a very lax QC on SATEMs with only a few rejected satellite thicknesses. The HRA forecasts based on the 11-layer satellite version showed a clear degradation relative to FEB 87 operations in some cases. In Fig. 11a the mean anomaly correlations are shown for 4 forecasts (same set as for the QC experiments) for Northern hemisphere.

The period was reassimilated using the 7-layer satellite data high resolution analysis and a similar 7-layer MRA system as control. The 7-layer analysis version has a more stringent QC on satellite thicknesses than the 11-layer version. The 11-layer HRA forecasts are clearly worse than the 11-layer MRA forecast beyond Day 4 in the Northern hemisphere (Fig. 11a). Much of this loss in skill is recovered by using the 7-layer satellite data analysis instead (Fig. 11b). The Northern hemisphere scores show clear improvement in the early range but still a loss of skill around day 5 to 6 compared to MRA.

The Southern hemisphere scores show a healthy improvement throughout the whole forecast range. Again, the 7-layer satellite system (Fig. 12 b) is much more favourable to the HRA scheme than the 11 layer satellite analysis (Fig. 12 a).

The strong forecast impact from the different versions of the analysis schemes is clearly evident from synoptic evaluation of the short and medium range forecasts. The forecasts are particularly sensitive to the analyses in the Eastern Pacific. Some forecasts show striking improvements locally over North America from improved use of satellite data and increased analysis resolution. Although there are several exciting forecasts demonstrating strong sensitivity to analyses only the experimentation with the October 87 storm will be discussed in detail.

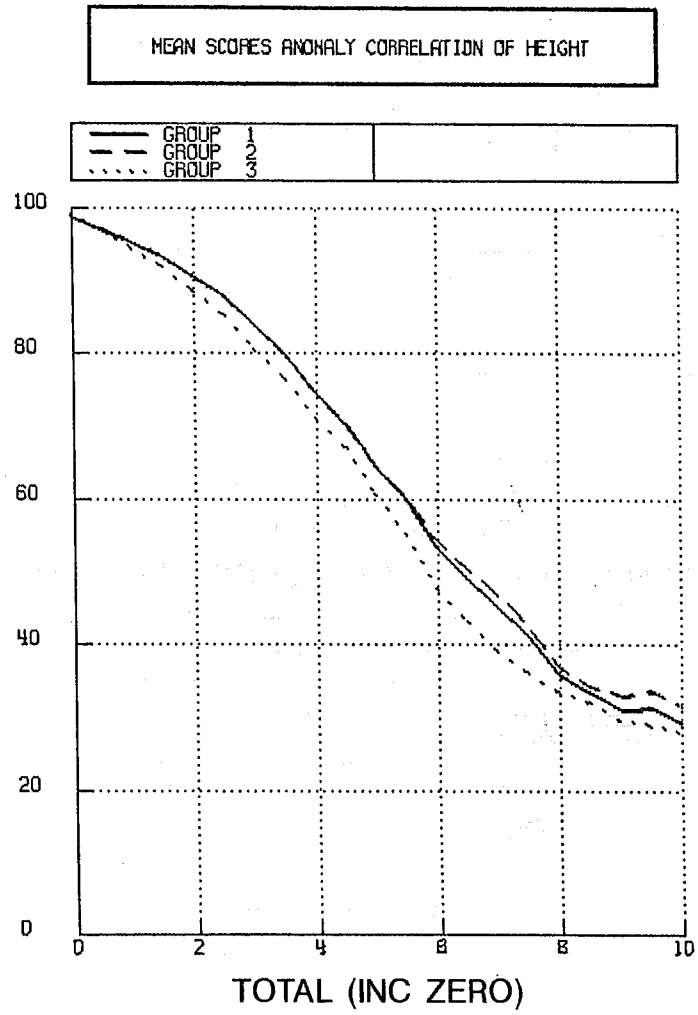


Fig. 10 Anomaly correlation for Southern hemisphere height. Mean over 4 cases. Solid line denotes tough QC, dashed line medium QC and dotted line loose QC.

a)

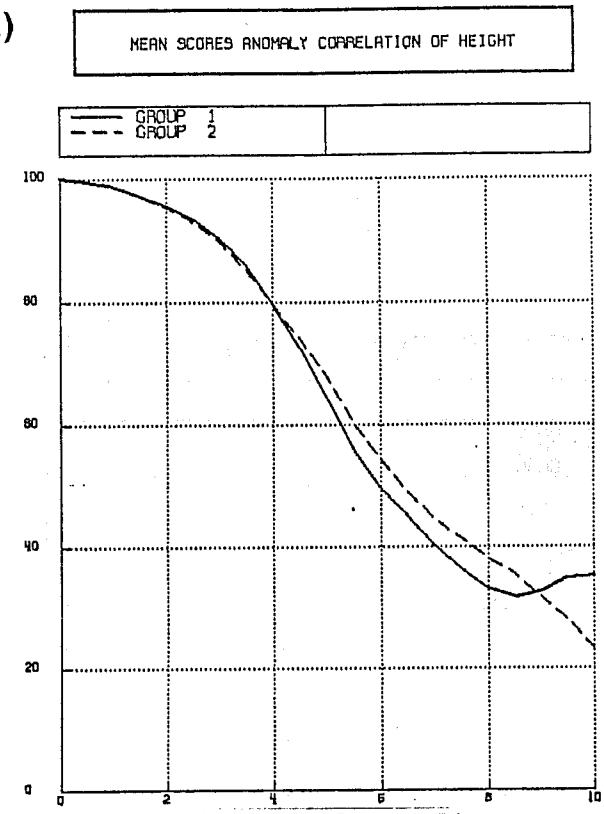


b)

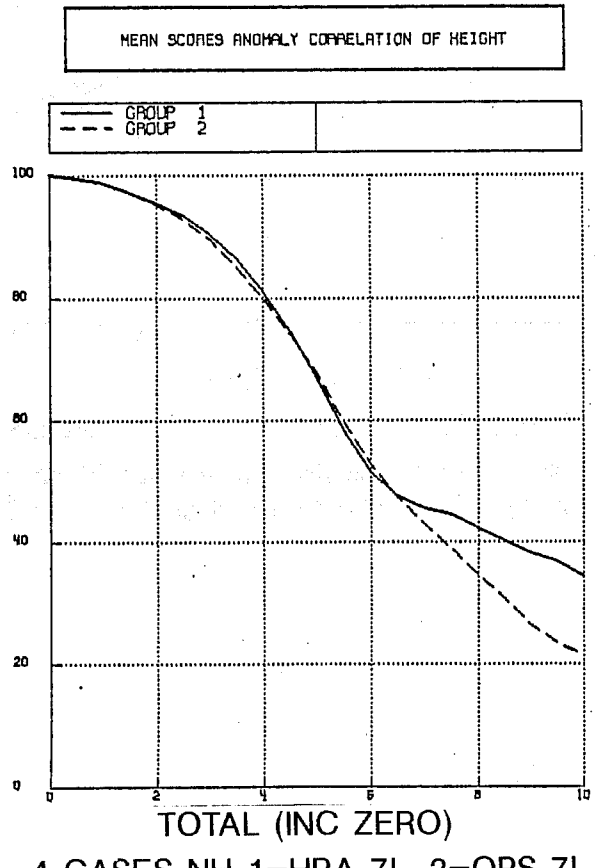


Fig. 11 Anomaly correlation of Northern hemisphere height. Mean over 4 cases. Part a compares 11 layer satellite HRA system (solid) with 11 layer MRA (dashed). Similarly part b for the 7 layer satellite systems.

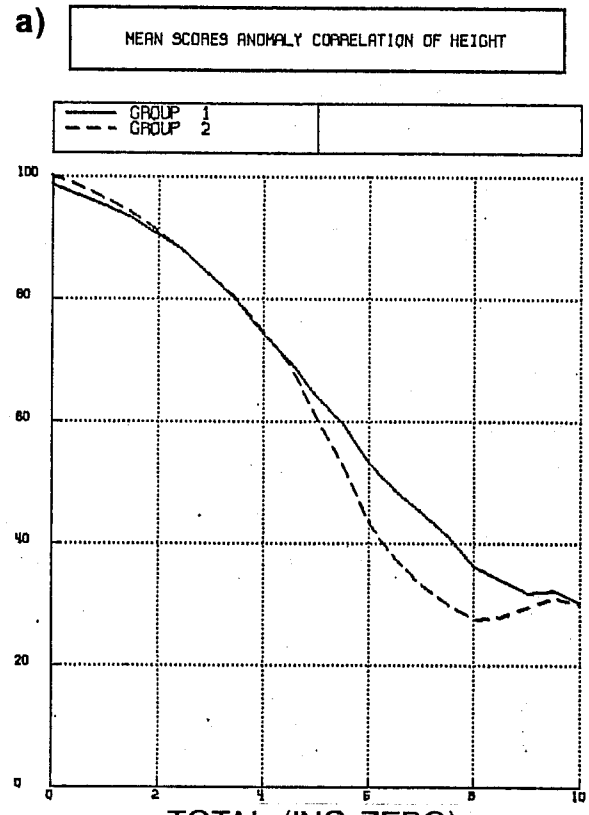


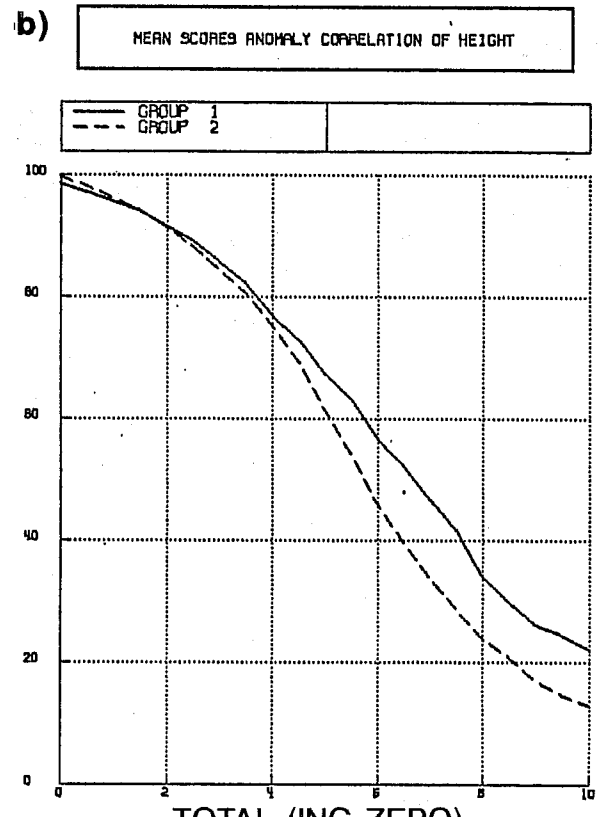


Fig. 12 Same as Fig. 11, but for Southern hemisphere.

## 4.3 October 87 storm

The most spectacular case of analysis and forecast impact to the effective analysis resolution is the October 87 storm. The assimilation of this storm exhibits several interesting features which are characteristic of intermittent analysis schemes. The HRA assimilation was started at 12 UTC on 12 October 87 to capture the upstream development of the storm.

The storm of 15-16 Ocober 1987 is reported in detail in the April 1988 issue of the Meterological Magazine. At midnight on 15 October 87 an area of low pressure extended from Bay of Biscay to 30 W (Figs. 13a and b). The HRA analysis (Fig. 13b) has a clearer indication of a cyclone at 30 W than the MRA analysis with a more westward position in HRA. From this time onwards the MRA and HRA analyses diverge rapidly. The HRA assimilation rapidly deepens the westernmost low and by 12 UTC on 15 October 87 an intense cyclone has developed in HRA (Fig. 14b). Very few surface reports were available in the vicinity of the low to aid the assimilation on intensity and position of the cyclone. Only a limited number of AIREP and SATOB reports influence the analysis. The MRA assimilation produces a different but equally possible solution given the available data. The MRA analysis is 11 hPa shallower than HRA and further to the east. It is quite obvious from the divergence of the two assimilations that the surface network of the Eastern Atlantic is too sparse to capture small scale cyclones.

The second assimilation problem occurs when the cyclone reaches coastal regions with good coverage of surface observations. A large mismatch between background field and observations as regards phase and amplitude leads to strong adjustment of mass and wind field thereby disrupting the smooth forecast evolution.

In extreme cases, the background has diverged too far from the "truth" because of lack of data causing the third problem, rejection of good data. The conditional first-guess test on surface pressure data (see Section 2.3.3) was devised to avoid rejections against a poor first-guess. In the assimilation of the October storm a good match between background and observations is achieved only after two analysis cycles with good data coverage.

The forecasts, 4 in total, show a consistent improvement over the corresponding MRA forecasts with respect to depth and position of the cyclone. The HRA forecasts from 14 October 12 UTC and 15 October 0 and 12 UTC all gave an accurate cyclone track, while the MRA forecasts failed miserably. The storm in the HRA forecasts moved over England to the North Sea, while the MRA forecasts moved the cyclone along the French coast to Belgium and Netherlands.

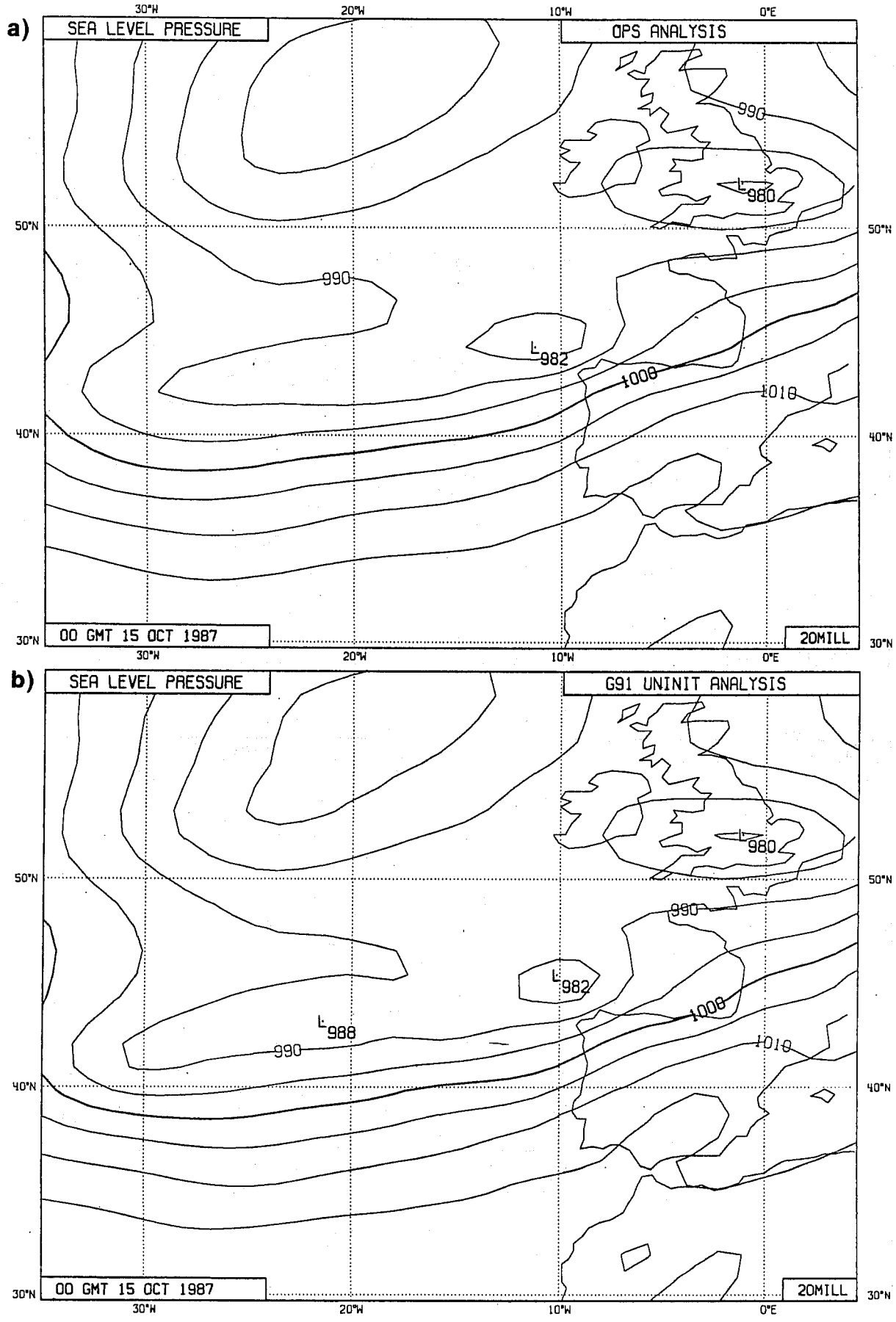


Fig. 13 Sea level pressure analyses at 15 October 1987 0 UTC by MRA system (a) and HRA system (b).

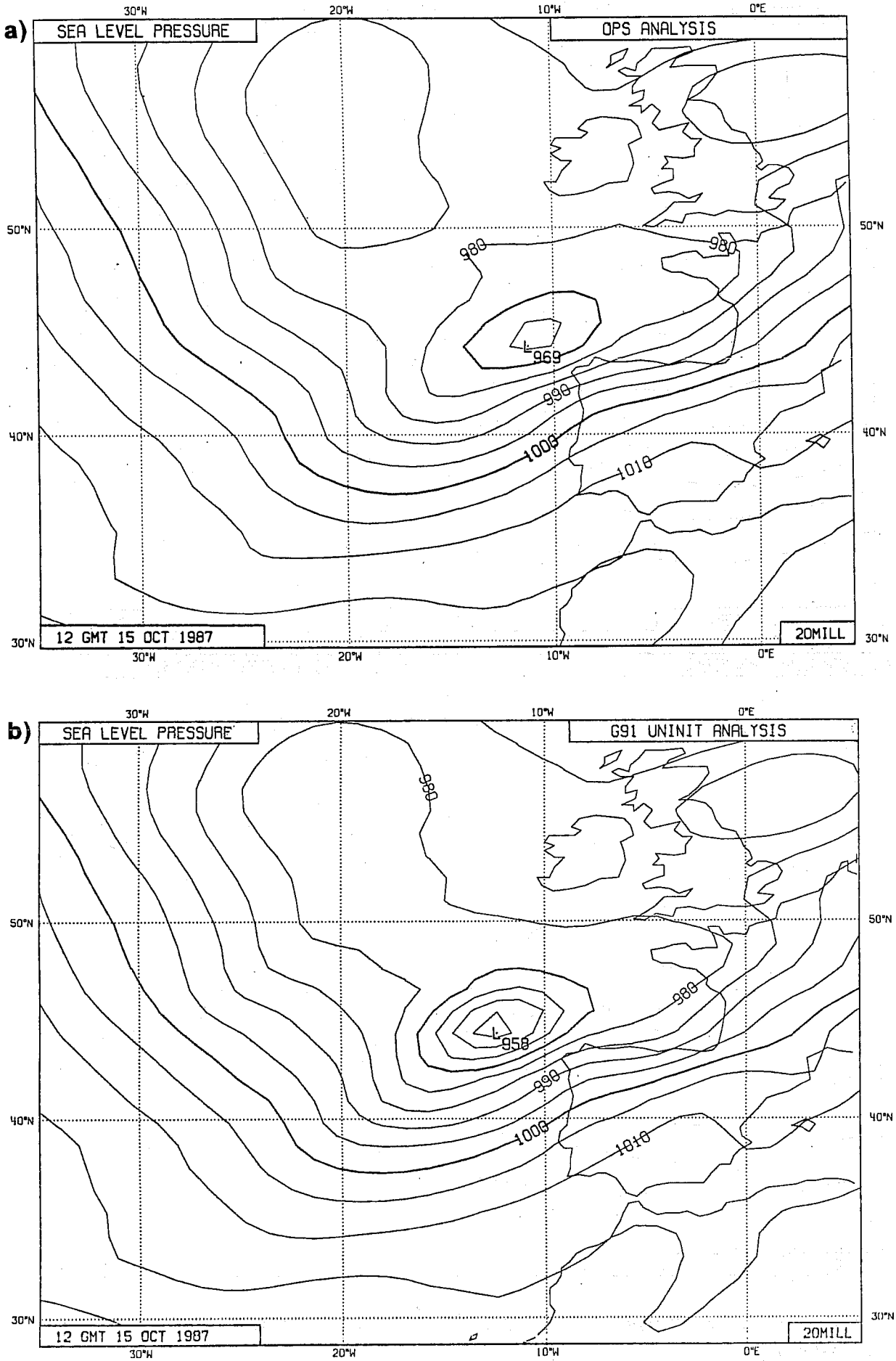


Fig. 14 Same as Fig. 13, but for 15 October 1987 12 UTC.

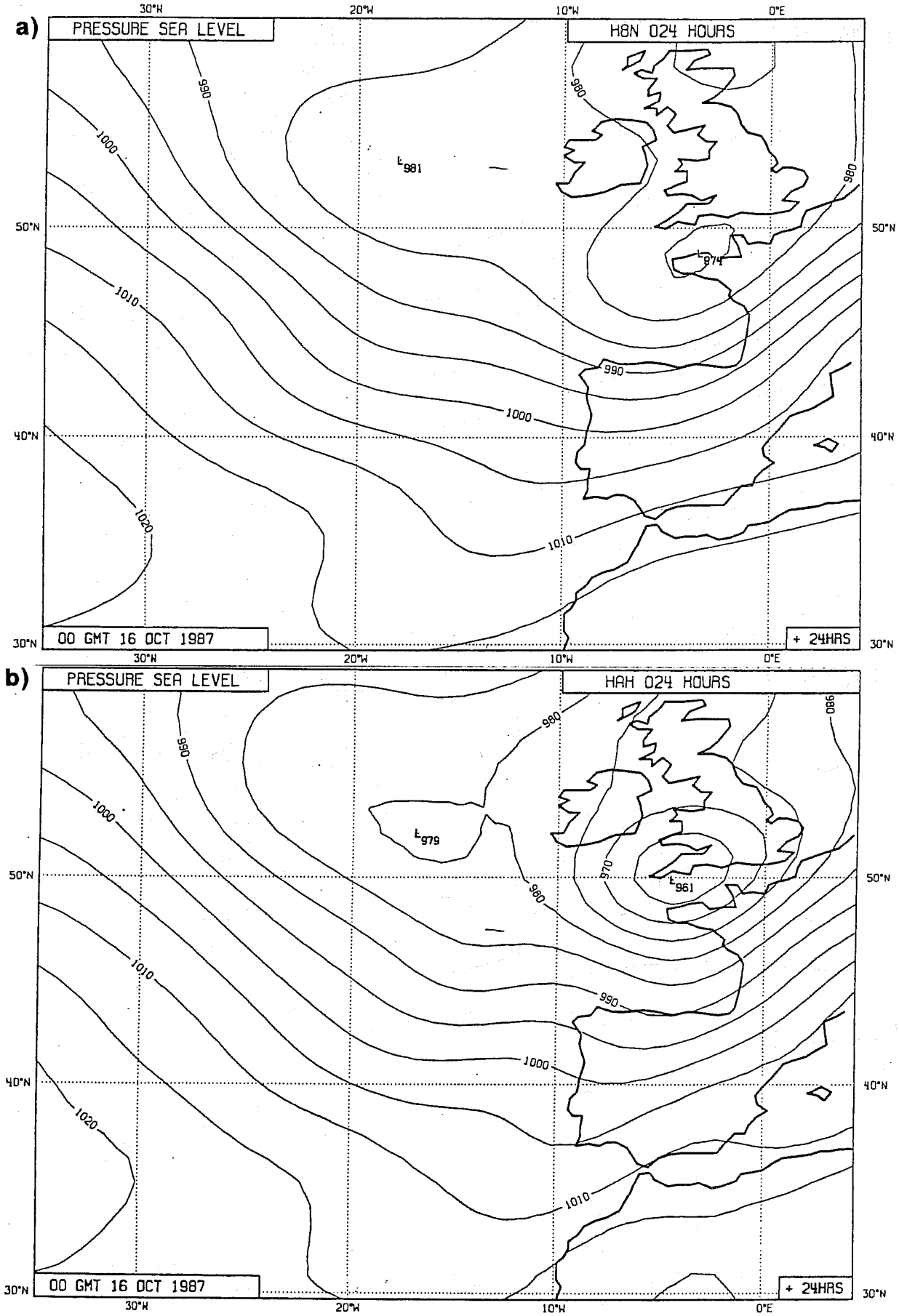


Fig. 15 24 hour forecast from MRA analysis (a) and HRA (b) valid at 16 October 87 0 UTC.

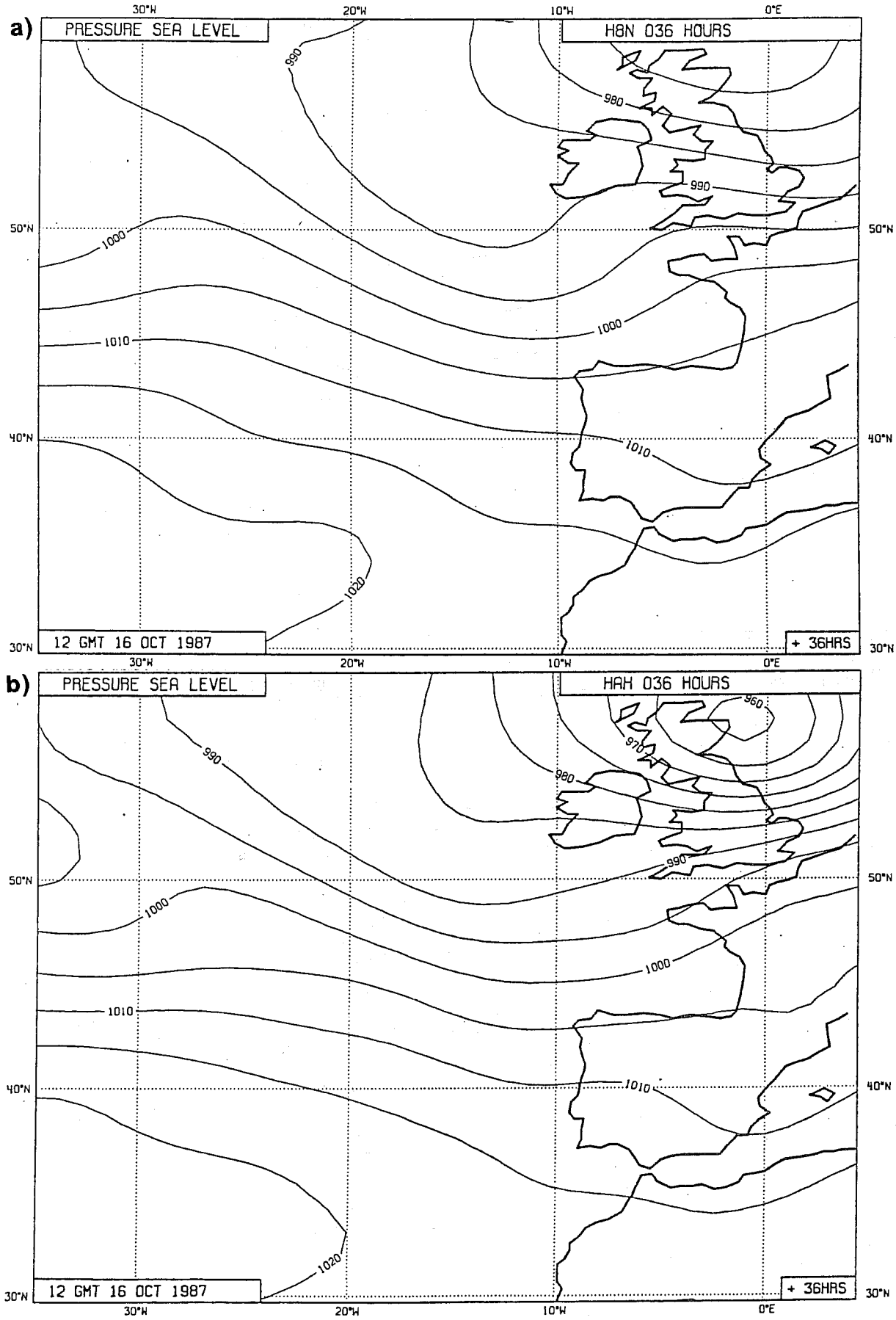


Fig. 16 Same as Fig. 15, but for 36 hour forecast valid at 16 October 87 12 UTC.

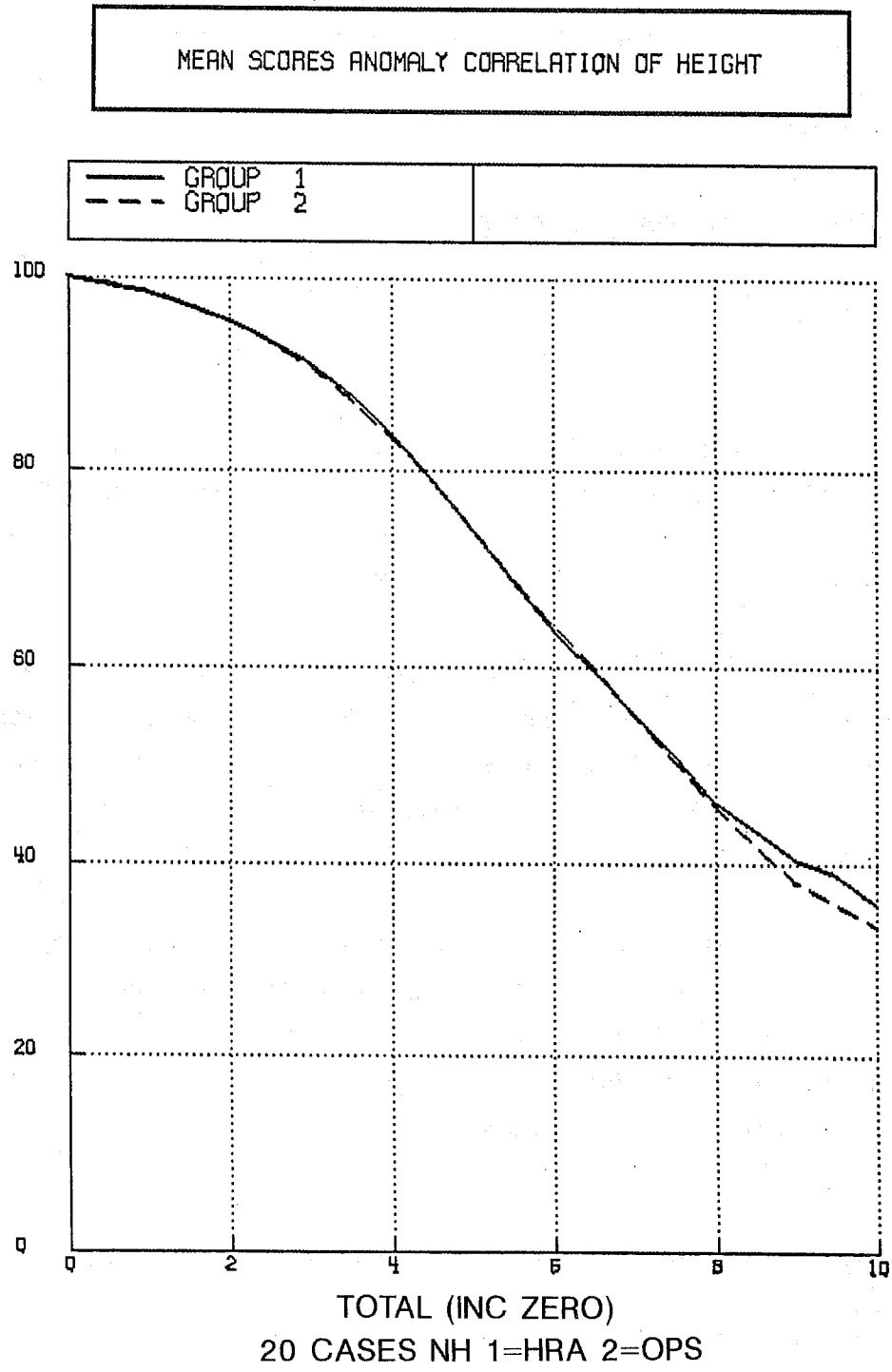


Fig. 17 Anomaly correlation of Northern hemisphere height. Mean over 20 cases. Solid denotes forecasts from HRA analyses and dashed from medium resolution analysis.

The depth of the low improved, in particular in the forecast from 0 UTC on 15 October. In the 24 hour forecast, valid at midnight on 16 October, there is a gain of 13 hPa over MRA (Fig. 15). The HRA forecast produces rather strong winds at the South Coast of England. In the MRA forecast the wind is very weak in southern England. Also, the westerly flow, 12 hours later, behind the cyclone is considerably stronger in the HRA forecast as compared to MRA (Fig. 16). The other HRA forecasts were less successful in predicting the intensity of the storm.

### 4.4 Assessment of forecast impact from HRA analyses

The final version of the HRA scheme has been tested on 20 different cases. 11 forecast cases have been run with the 11 layer satellite version and 9 cases with the current 7 layer satellite scheme.

The average scores for the Northern hemisphere are shown in Fig. 17. An improvement of the forecast skill is evident in the short and early medium range. At Day 5 and 6 the MRA and HRA systems are equal. Experimentation suggests that this drop in skill might be caused by stronger response to bad satellite sounding data in HRA than MRA.

These results can be stated in another way. The 11-layer satellite data scheme is the least favourable to the HRA system, while the best one is the 7-layer satellite data analysis with tough QC. It may then be argued that the ensemble scores presented underestimate the skill of the forecasts from HRA, as many of them have not been run with the most favourable satellite scheme.

At Day 3 most forecasts show an increased skill (even when verified against MRA analyses); some of which like 1 February 87 is distinctly better already very early in the forecast (See scatterdiagrams, Fig. 18). At Day 5 (Fig. 19) there is no gain in skill by the HRA forecasts over the MRA forecasts. The skill in the Southern hemisphere (Fig. 20) exhibits the same variation as in the Northern Hemisphere with the smallest gain around Day 5. The scatter of the forecast skill is very large (not shown).

## 5. ON-GOING WORK ON IMPROVING VERTICAL AND TEMPORAL ANALYSIS RESOLUTION

Currently, only one height and one wind report is used for each model layer with preference given to mandatory pressure level data. Empirical studies on the structure of the short-range forecast errors (HL) show that the height and the wind vertical correlations are distinctly different with the wind correlations being quite narrow. The assumption of horizontal and vertical separability of the forecast error correlations is mainly based on computational arguments and lack of vertical resolution of the analysis

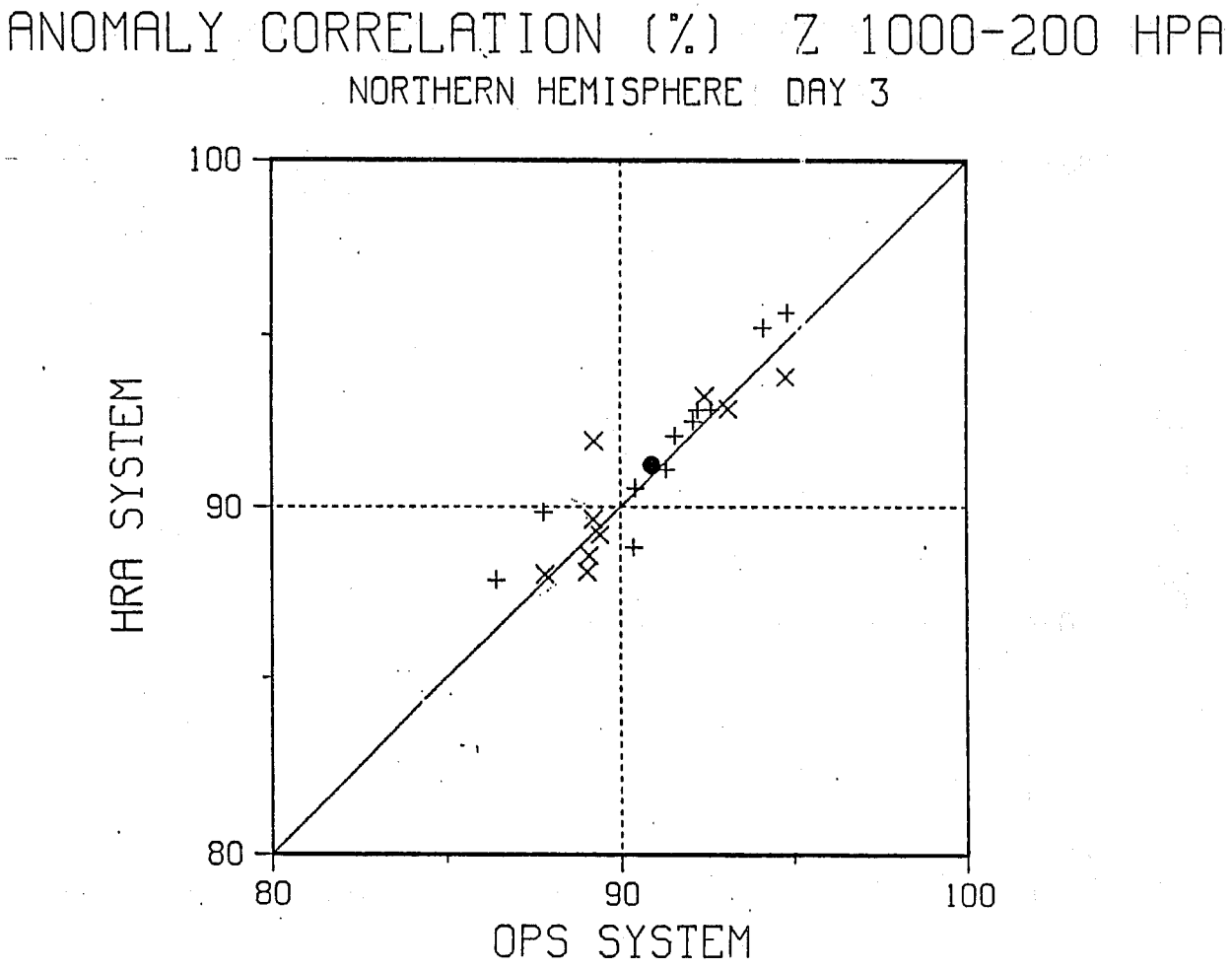


Fig. 18 Scatterdiagram of anomaly correlations of 1000 - 200 hPa height comparing forecasts from HRA with forecasts from MRA analyses at Day 3 for Northern hemisphere. + denotes analyses with 11 layer satellites and x analyses with 7 layer satellites. The average correlation is indicated by a filled circle.

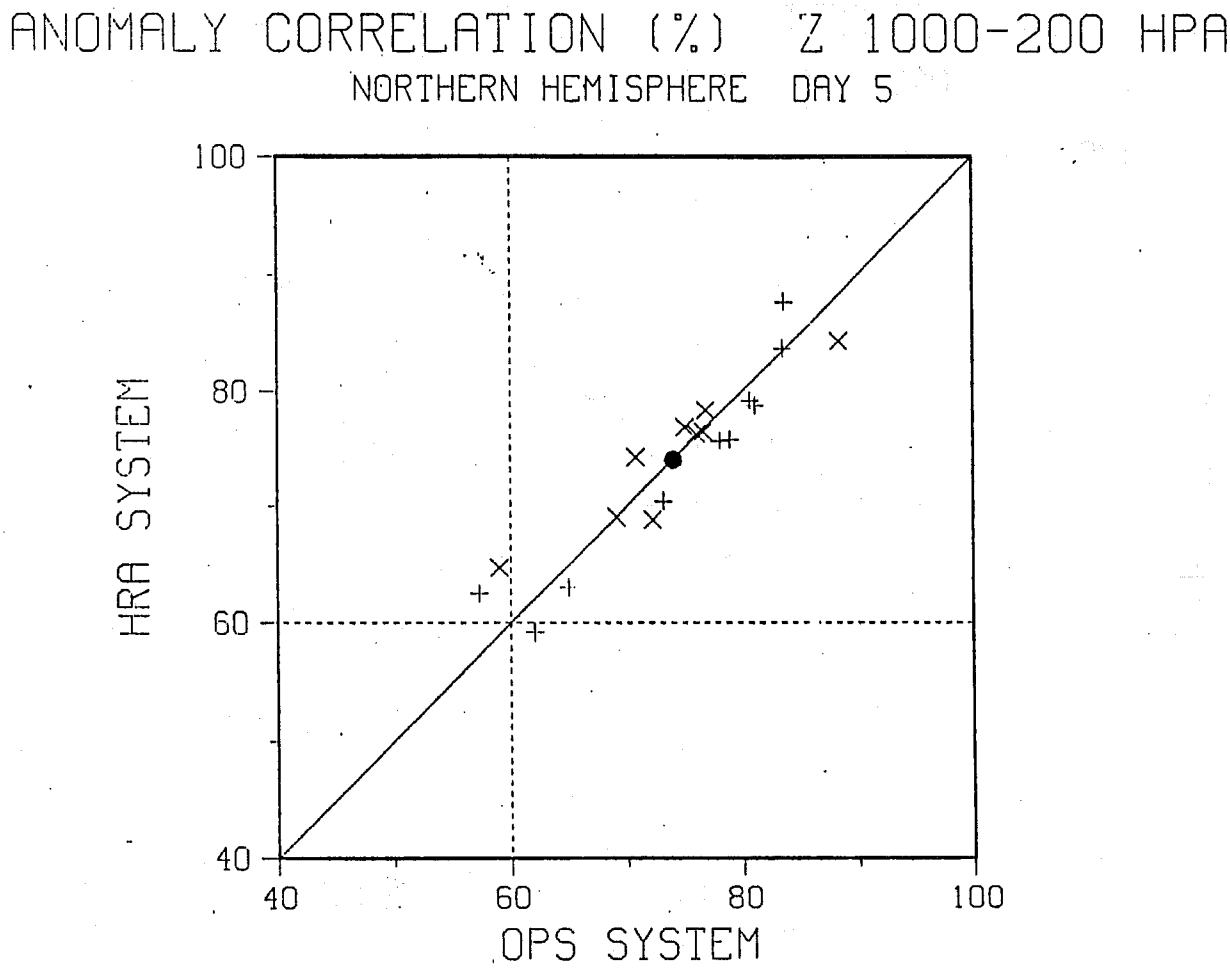


**Fig. 19 Same as Fig. 18, but for Day 5.**

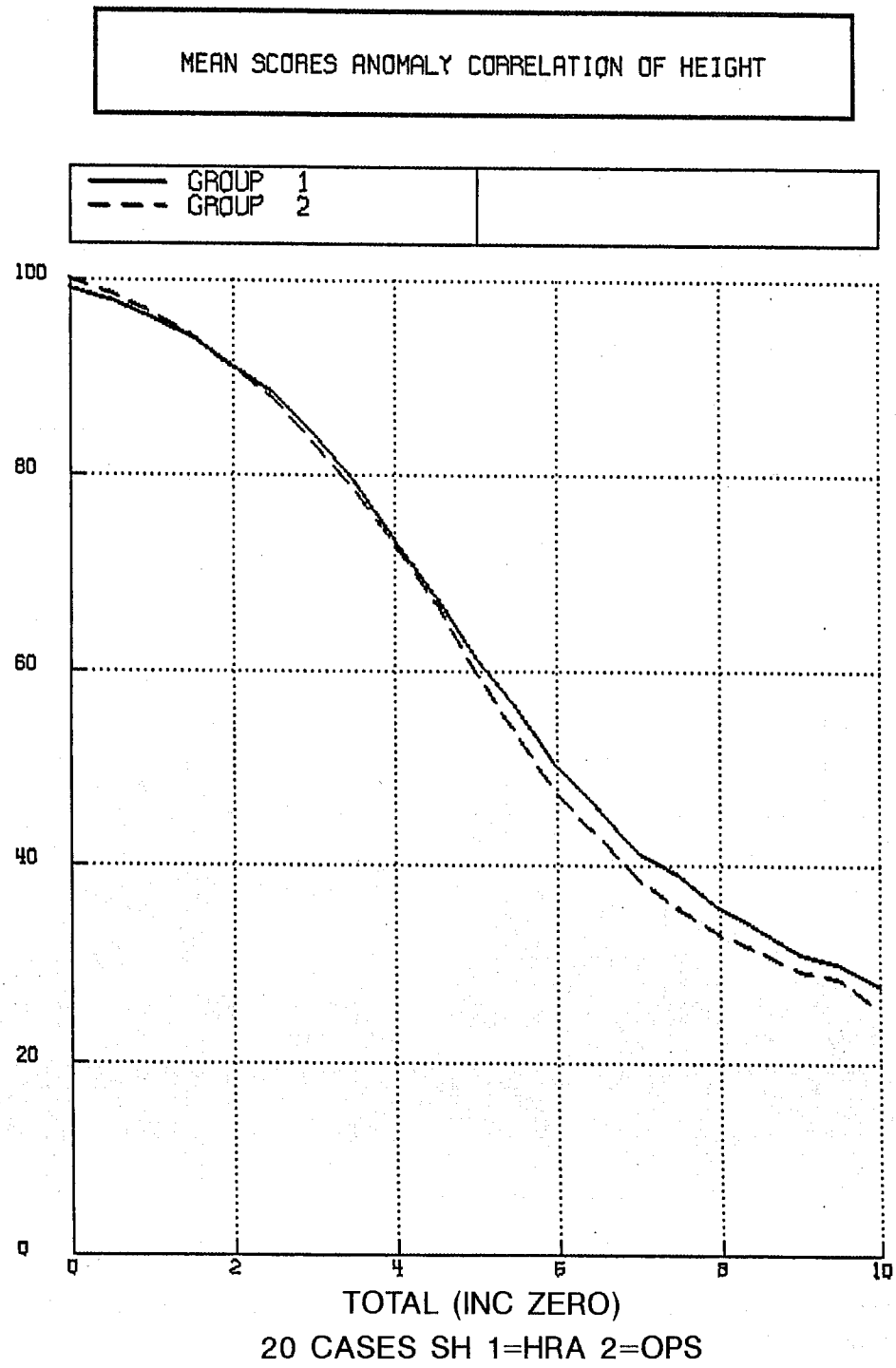


Fig. 20 Same as Fig. 17, but for Southern hemisphere.

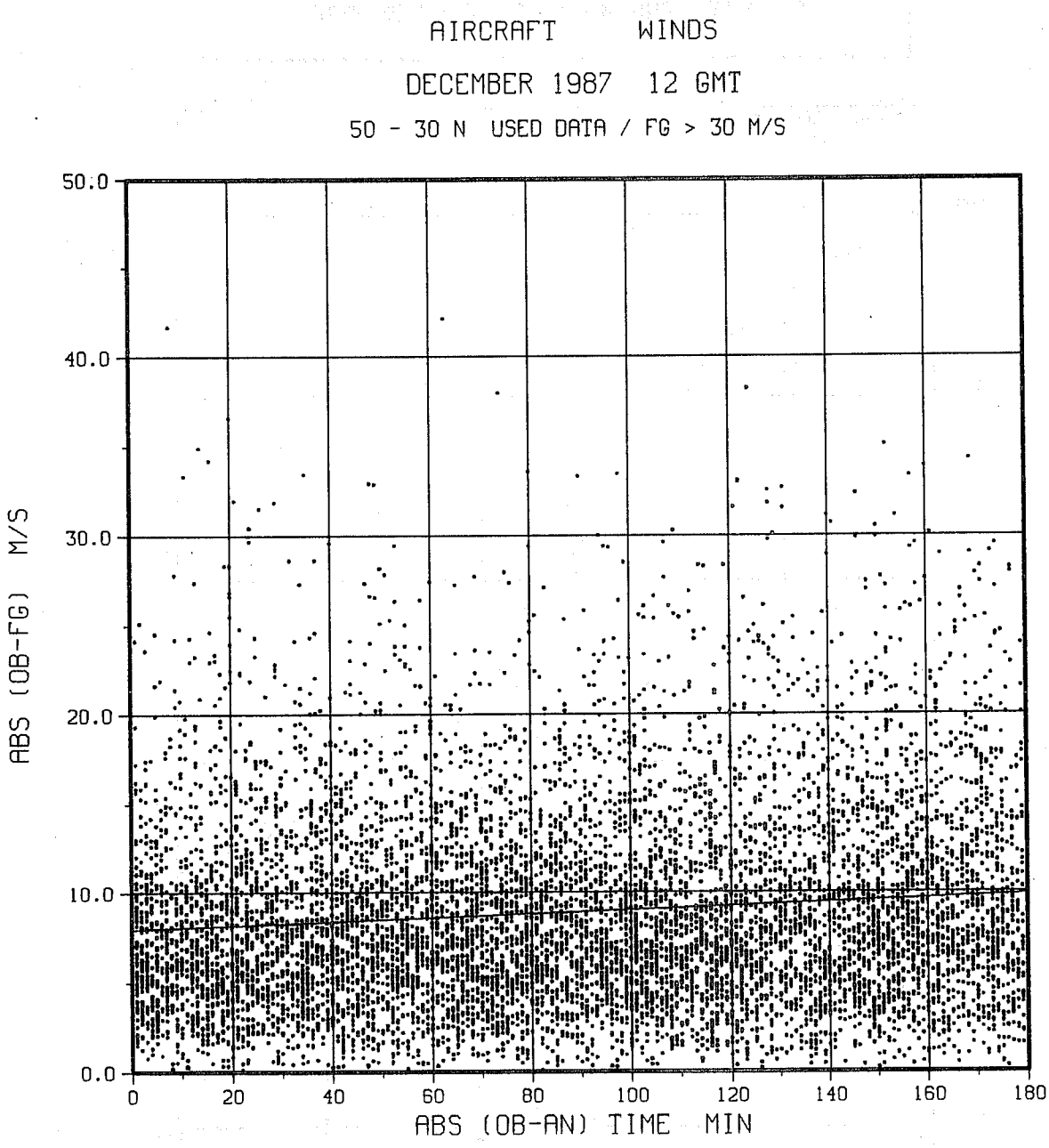


Fig. 21 Scatterdiagram of difference between aircraft wind reports and six hour forecast as function of absolute value of time difference between time of report and analysis time for background wind speeds exceeding 30 m/s.

projection grid, i.e. the forecast model. Higher model resolution and use of more information from sondes are necessary prerequisites for use of sharper vertical wind correlations. Preliminary results with a 31 level model used in data assimilation are encouraging (Simmons and Undén, pers. comm.).

As the errors of the six hour forecast are reduced and as the effective spatial analysis resolution is increased, the error arising from the mismatch between observation and analysis times becomes serious.

The operational practice of the ECMWF data assimilation is to use all available observations within 3 hours from the analysis time. In case of surface stations reporting more than once in such a six hour period, the observation closest to the analysis time is used in preference to other observations from the same station. When available the surface pressure tendency is used to correct the pressure to the analysis time. However, a large number of critical observations, like aircraft and satellite soundings are used without temporal correction. The temporal error has been estimated from aircraft reports (Fig. 21). The rms value of the difference between observed value and background has been stratified according to time difference between report and background. A linear regression line of the vector wind difference as function of time difference has been determined.

The difference between background and observations consists of three independent error sources: observation, forecast and temporal mismatch errors. From observations made at the analysis time we obtain the sum of the observation and forecast error variances. By subtracting these from the observation-minus-background variance for data separated in time from the analysis time, we can estimate the temporal error. The temporal error is 6.1 m/s (vector wind) for data separated by 3 hours from the background time. The observation and forecast errors are, if assumed equal, 5.6 m/s. At one hour separation the temporal error is 3.4 m/s and at two hours 4.8 m/s. Already for observations separated by one hour is the temporal error quite significant.

## 6. CONCLUSIONS

The HRA scheme gives more detailed analyses than the MRA scheme, in particular of jets. The forecasts run from HRA assimilations show very strong sensitivity to the initial state. There is a clear improvement of the forecast skill in the short range up to day 4, while some forecasts deteriorate in the medium range, especially around day 5 to 6. Some forecasts show spectacular gains in predicting intense storms in the short range.

By its very nature the HRA scheme extracts more information from the observation, which increases its sensitivity to errors in the data. Perhaps, the strongest signal to emerge

from the HRA experimentation is the analysis and forecast sensitivity to quality control of observations. HRA forecasts which are less skilful than the corresponding MRA forecasts are usually associated with satellite data problems. The filtering properties of the MRA scheme are so strong that noise in the data are suppressed as well as any extreme meteorological signal. Improvements in the effectiveness of QC will require more independent information (position, time continuity, recent quality) and better methods.

Further benefits are expected from increased vertical model resolution and removal of the mismatch between observation and background times.

References

Andersson, E. and Hollingsworth, A. 1988 Typhoon bogus observations in the ECMWF data assimilation system. ECMWF Tech. Memo. No. 148, 25 pp.

Bengtsson, L. 1988 On the growth of errors in data assimilation systems. These Proceedings.

Böttger, H. and Radford A. 1988 Monitoring of satellite data. These Proceedings.

Courtier, P. 1988 Four dimensional variational assimilation: shallow water. These Proceedings.

Gandin, L. 1988 Complex quality control of meteorological observations. Mon.Wea.Rev., 116, 1137-1156.

Hollingsworth, A. and Lönnberg, P. 1986 The statistical structure of short-range forecast errors as determined from radiosonde data. Part I: The wind field. Tellus, 38A, 111-136.

Hollingsworth, A. and Lönnberg, P. 1989 The verification of objective analyses: Diagnostics of analysis system performance. Met. Atm.Phys., 40, 3-27.

Jarraud, M., Simmons, A.J. and Kanamitsu, M. 1985 Development of the high resolution model. ECMWF Tech. Memo. No. 107, 61 pp.

Kelly, G. 1988 Satellite temperature sounding. These Proceedings.

Lönnberg, P. and Hollingsworth, A. 1986 The statistical structure of short-range forecast errors as determined from radiosonde data. Part II: The covariance of height and wind errors. Tellus, 38A, 137-161.

Lönnberg, P., Pailleux, J. and Hollingsworth, A. 1986 The new analysis system. ECMWF Tech. Memo. No. 125, 21 pp.

Lönnberg, P and Shaw, D. (Eds.) 1987 ECMWF Data Assimilation Scientific Documentation. Research Manual 1.

Lorenc, A.C. 1981 A global three-dimensional multivariate statistical interpolation scheme. Mon.Wea.Rev., 109, 701-721.

Lorenc, A.C. and Hammon, O. 1988 Objective quality control of observations using Bayesian methods. Theory, and a practical implementation. Q.J.R.Met.Soc., 114, 515-543.

Pailleux, J., Kelly, G., Flobert, J-F. and Andersson, E. 1988 Current work at ECMWF on the use of satellite data. These Proceedings.

Shaw, D., Lönnberg, P. and Hollingsworth, A. 1984 The 1984 revision of the ECMWF analysis system. ECMWF Tech. Memo. No. 92, 69 pp.

Shaw, D.B., Lönnberg, P., Hollingsworth, A. and Undén, P. 1987 Data assimilation: The 1984/85 revisions of the ECMWF mass and wind analysis. Q.J.R.Met.Soc., 113, 533-566.

Talagrand, O. 1988 Four dimensional variational analysis. These Proceedings.

Undén, P. 1988 Tropical data assimilation and analysis of divergence. These Proceedings.